Cell Reports
Article

Critical Role for Mast Cell Stat5 Activity in Skin Inflammation

Tomoaki Ando,[1] Wenbin Xiao,[1,10] Peisong Gao,[2] Siavash Namiranian,[3] Kenji Matsumoto,[4] Yoshiaki Tomimori,[1,11] Hong Hong,[1,10] Hirotaka Yamashita,[1] Miho Kimura,[1,12] Jun-ichi Kashiwakura,[5] Tissa R. Hata,[6] Kenji Izuhara,[7] Michael F. Gurish,[8] Axel Roers,[9] Nicholas M. Rafaels,[2] Kathleen C. Barnes,[2] Colin Jamora,[3] Yuko Kawakami,[1] and Toshiaki Kawakami[1,5,*]
[1]Division of Cell Biology, La Jolla Institute for Allergy and Immunology, La Jolla, CA 92037, USA
[2]Division of Allergy and Clinical Immunology, Johns Hopkins University, Baltimore, MD 21224, USA
[3]Department of Bioengineering, University of California San Diego, La Jolla, CA 92093, USA
[4]Department of Allergy and Immunology, National Research Institute for Child Health and Development, Tokyo 157-8535, Japan
[5]Laboratory for Allergic Disease, RIKEN Center for Integrative Medical Sciences (IMS-RCAI), Yokohama 230-0045, Japan
[6]Division of Dermatology, Department of Medicine, University of California San Diego, La Jolla, CA 92037, USA
[7]Division of Medical Biochemistry, Department of Biomolecular Sciences and Department of Laboratory Medicine, Saga Medical School, Saga 849-85-01, Japan
[8]Department of Medicine, Brigham and Women's Hospital, Boston, MA 02115, USA
[9]Institute for Immunology, University of Technology Dresden, Medical Faculty Carl-Gustav Carus, 01307 Dresden, Germany
[10]Present address: Department of Pathology, University Hospitals Case Medical Center, Case Western Reserve University, Cleveland, OH 44106, USA
[11]Present address: Asubio Pharma, Kobe 650-0047, Japan
[12]Present address: Department of Rheumatology and Infectious Diseases, Kitasato University School of Medicine, Sagamihara 252-0374, Japan
*Correspondence: toshi@lji.org
http://dx.doi.org/10.1016/j.celrep.2013.12.029

SUMMARY

Atopic dermatitis (AD) is a chronic inflammatory skin disease. Here, we show that phospholipase C-β3 (PLC-β3)-deficient mice spontaneously develop AD-like skin lesions and more severe allergen-induced dermatitis than wild-type mice. Mast cells were required for both AD models and remarkably increased in the skin of *Plcb3*$^{-/-}$ mice because of the increased Stat5 and reduced SHP-1 activities. Mast cell-specific deletion of *Stat5* gene ameliorated allergen-induced dermatitis, whereas that of *Shp1* gene encoding Stat5-inactivating SHP-1 exacerbated it. PLC-β3 regulates the expression of periostin in fibroblasts and TSLP in keratinocytes, two proteins critically involved in AD pathogenesis. Furthermore, polymorphisms in *PLCB3*, *SHP1*, *STAT5A*, and *STAT5B* genes were associated with human AD. Mast cell expression of PLC-β3 was inversely correlated with that of phospho-STAT5, and increased mast cells with high levels of phospho-STAT5 were found in lesional skin of some AD patients. Therefore, STAT5 regulatory mechanisms in mast cells are important for AD pathogenesis.

INTRODUCTION

Atopic dermatitis (AD) is a chronic or chronically relapsing inflammatory skin disease. Although the etiology of AD is not completely understood, numerous studies suggest that immune dysregulation and impaired skin barrier function underlie the disease (Bieber, 2008; Boguniewicz and Leung, 2011). Epidermal overexpression of thymic stromal lymphopoietin (TSLP), a T_H2-promoting cytokine (Liu, 2006; Ziegler and Artis, 2010), seems to be a major mechanism for AD development (Li et al., 2005; Soumelis et al., 2002; Yoo et al., 2005). Periostin, an α_v integrin-interacting matricellular protein (Hamilton, 2008; Ruan et al., 2009), recently emerged as another mediator for AD that induces TSLP production from keratinocytes (Masuoka et al., 2012). A mouse AD model (Spergel et al., 1998) induced by epicutaneous treatment of ovalbumin revealed the involvement of T_H2, T_H1, and T_H17 cytokines and other factors (Jin et al., 2009a). Another model (Kawakami et al., 2007) induced by allergen (extract of *Dermatophagoides farinae*, Der f) and staphylococcal enterotoxin B (SEB) also showed the requirement of mast cells and T cells as well as TSLP receptor (TSLPR) (Ando et al., 2013).

Phospholipase C (PLC) is a family of enzymes that catalyze the hydrolysis of phosphatidylinositol 4,5-bisphosphate in order to generate diacylglycerol and inositol 1,4,5-trisphosphate (Suh et al., 2008). Independent of its enzymatic activity, PLC-β3 inhibits the proliferation of hematopoietic stem cells (HSCs)

Cell PRESS
Open ACCESS

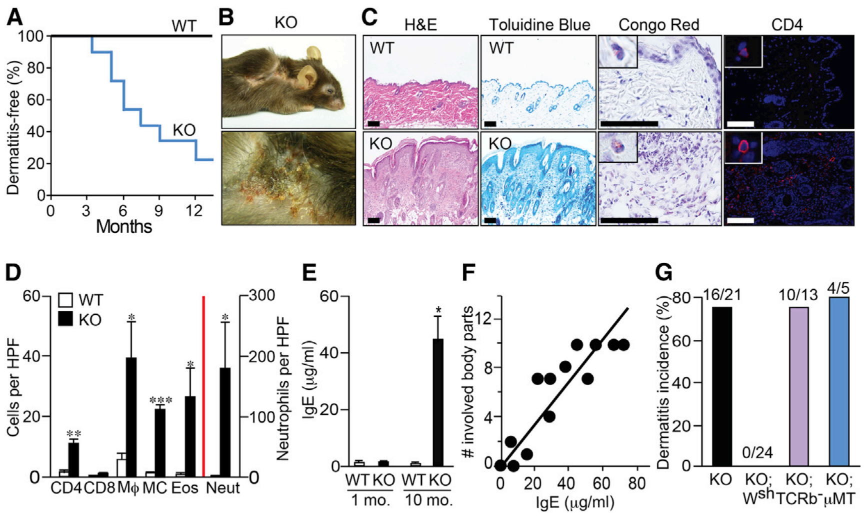

Figure 1. *Plcb3*$^{-/-}$ Mice Spontaneously Develop AD-like Skin Lesions in a Mast Cell-Dependent Manner

(A) Kaplan-Meier plots for dermatitis development in *Plcb3*$^{-/-}$ mice (n = 21).

(B) Note the eczematous skin lesions and hair loss in periocular areas, cheeks, ears, neck, and flanks in a 10-month-old *Plcb3*$^{-/-}$ mouse.

(C) Histology of healthy (WT) and skin lesions (*Plcb3*$^{-/-}$) in ear. Scale bar, 100 μm.

(D) Graphic representation of histological analysis of ear skin lesions of 8- to 10-month-old WT and *Plcb3*$^{-/-}$ mice. Neutrophils (Neut), eosinophils (Eos), and mast cells (MC) were enumerated in H&E-, Congo-red- and Toluidine-blue-stained preparations, respectively. Immunofluorescence staining was performed to detect CD4$^+$, CD8$^+$, and F4/80$^+$ (Mϕ) cells. Data represent mean ± SEM. *p < 0.05, **p < 0.01, ***p < 0.001 versus WT mice by Student's t test. Similar results were obtained in lesional skin in cheeks and neck (data not shown). HPF, high-power field.

(E) Serum IgE levels were increased in 8- to 10-month-old *Plcb3*$^{-/-}$ mice. Data represent mean ± SEM.

(F) Correlation between serum IgE levels and numbers of body parts with skin lesions (see the legend for B for eczematous body parts). r^2 = 0.78, p < 0.0001, Pearson's correlation.

(G) Incidence of skin lesions in *Plcb3*$^{-/-}$ (KO), *Plcb3*$^{-/-}$;*Kit*$^{W\text{-}sh/W\text{-}sh}$ (KO;W^{sh}), *Plcb3*$^{-/-}$;*TCRb*$^{-/-}$ (*KO;TCRb*$^-$) and *Plcb3*$^{-/-}$;*μMT/μMT* (*KO;μMT*) mice for 12 months.

Results in (E) and (F) are representative of two independent experiments using three to six mice per group. See also Figure S1.

and myeloid cells by interacting with SH2-domain-containing protein phosphatase 1 (SHP-1) and signal transducer and activator of transcription 5 (Stat5) and augmenting the dephosphorylating activity of SHP-1 toward Stat5, leading to the inactivation of Stat5 (Xiao et al., 2009).

The present study demonstrated that PLC-β3-deficient mice spontaneously develop AD-like skin lesions. We investigated the cellular and molecular mechanisms for spontaneous and allergen-induced AD-like dermatitis in *Plcb3*$^{-/-}$ mice and their clinical relevance to human AD.

RESULTS

PLC-β3-Deficient Mice Spontaneously Develop Mast Cell-Dependent AD-like Dermatitis

Young (4- to 10-week-old) *Plcb3*$^{-/-}$ mice displayed no obvious abnormalities in their phenotype. By contrast, a majority of older mice developed eczematous skin lesions and hair loss in their periocular areas, cheeks, ears, neck, and trunk (Figures 1A and 1B). The lesions showed hyperkeratosis, thickened epidermis and dermis, and infiltration of T cells, mast cells, macrophages, eosinophils, and neutrophils in the dermis (Figures 1C and 1D). Eczematous *Plcb3*$^{-/-}$ mice had high levels of serum immunoglobulin (Ig) E and IgG1, whereas dermatitis-free young *Plcb3*$^{-/-}$ mice had low IgE levels (Figures 1E and S1A). There was a good correlation between IgE levels and numbers of the involved body parts (Figure 1F). Transepidermal water loss (TEWL) increased only after dermatitis development (Figure S1B), suggesting that skin barrier function was not primarily impaired in *Plcb3*$^{-/-}$ mice.

No *Plcb3*$^{-/-}$;*Kit*$^{W\text{-}sh/W\text{-}sh}$ mice (n = 24) deficient in mast cells developed skin lesions during an observation period of 12 months (Figure 1G). By contrast, skin lesions were observed in a majority of αβ T cell-deficient *Plcb3*$^{-/-}$ (*Plcb3*$^{-/-}$;*TCRb*$^{-/-}$) mice and B cell-deficient *Plcb3*$^{-/-}$;*μMT/μMT* mice. These results suggest that mast cells, but not αβ T or B cells, are indispensable for the spontaneous development of skin lesions in *Plcb3*$^{-/-}$ mice.

Plcb3$^{-/-}$ Mice Develop Severe Allergen-Induced Dermatitis

Der f/SEB-induced dermatitis is dependent on mast cells and T cells, but not B cells or eosinophils (Ando et al., 2013). Epicutaneous treatment with Der f and SEB of young (5- to 11-week-old) *Plcb3*$^{-/-}$ mice, which did not show any skin lesions before experiment, induced more severe skin lesions with thicker epidermis and dermis and higher levels of mast cell and neutrophil infiltration, compared to WT mice (Figures 2A–2E). Although Der f/SEB treatment increased serum levels of IgE and IgG1, some of which recognized Der f antigens, their levels were comparable in WT and *Plcb3*$^{-/-}$ mice (Figures S2A and S2B). As shown previously (Ando et al., 2013), mast cell-deficient *Kit*$^{W\text{-}sh/W\text{-}sh}$ mice showed less severe Der f/SEB-induced skin lesions than did WT mice. Mast cell deficiency also resulted in less severe skin lesions in Der f/SEB-treated *Plcb3*$^{-/-}$;*Kit*$^{W\text{-}sh/W\text{-}sh}$ mice, compared to *Plcb3*$^{-/-}$ mice (Figures 2F and 2G). Moreover, engraftment of *Plcb3*$^{-/-}$ bone-marrow-derived mast cells (BMMCs) into the back skin of *Plcb3*$^{-/-}$;*Kit*$^{W\text{-}sh/W\text{-}sh}$ mice restored the severity of Der f/SEB-induced dermatitis to levels in *Plcb3*$^{-/-}$ mice (Figures 2F–2H). Therefore, similar to spontaneous dermatitis in *Plcb3*$^{-/-}$ mice, mast cells contribute substantially to the development of Der f/SEB-induced dermatitis in these mice. Consistent with increased Der f-specific IgE levels in WT and *Plcb3*$^{-/-}$ mice, FcεRI-deficient mice exhibited

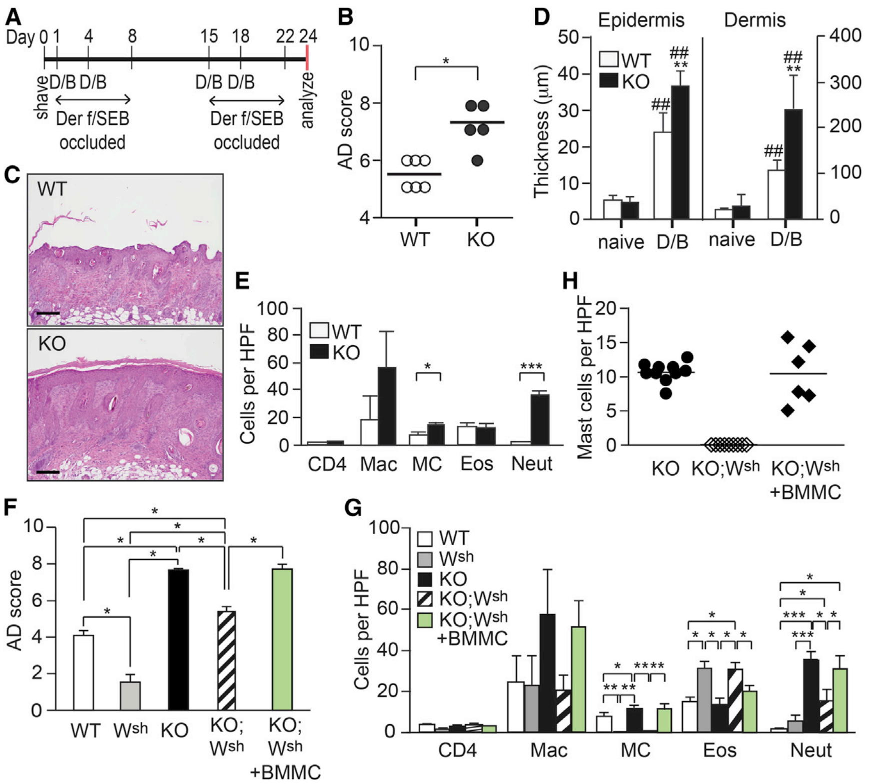

Figure 2. Mast Cells Significantly Contribute to the Increased Severity of Der f/SEB-Induced Skin Lesions in *Plcb3*$^{-/-}$ Mice

(A) AD-like skin lesions were induced as described previously (Kawakami et al., 2007). D/B, treatment with Der f and SEB. The periods when Der f/SEB-treated back skin is occluded with Tegaderm are also shown.

(B) AD scores on day 24 with WT and *Plcb3*$^{-/-}$ mice.

(C) H&E staining of lesional skins in WT and *Plcb3*$^{-/-}$ (KO) mice.

(D) Thicknesses of epidermis and dermis at basal and Der f/SEB (D/B)-treated levels were measured on H&E-stained lesional skins. Results in (B)–(D) are representative of three independent experiments using five to eight mice per group.

(E) Histologic analysis of Der f/SEB-induced dermatitis.

(F and G) Dermatitis was induced in WT, *Kit*$^{W\text{-}sh/W\text{-}sh}$ (Wsh), *Plcb3*$^{-/-}$ (KO) and *Plcb3*$^{-/-}$;*Kit*$^{W\text{-}sh/W\text{-}sh}$ (KO;Wsh) mice. A group of *Plcb3*$^{-/-}$;*Kit*$^{W\text{-}sh/W\text{-}sh}$ mice received BMMCs derived from *Plcb3*$^{-/-}$ mice 6 weeks before Der f/SEB treatment. (F) AD scores on day 24. (G) Histologic analysis of dermatitis. Data represent mean ± SD. *$p < 0.05$, **$p < 0.01$, ***$p < 0.001$ versus WT mice or indicated pairs by Student's t test or ANOVA; ##, $p < 0.01$ versus naive mice.

(H) Mast cells were quantified on Toluidine-blue-stained skin tissues. HPF, high-power field.

Results in (F)–(H) are representative of two independent experiments using six mice per group. See also Figure S2.

less severe skin lesions in *FceRIa*$^{-/-}$ and *FceRIa*$^{-/-}$;*Plcb3*$^{-/-}$ mice than the respective control FcεRI-sufficient mice (Figure S2C). These results indicate that FcεRI is required for full-blown allergen-induced dermatitis.

Plcb3$^{-/-}$ Mast Cells Are Hypersensitive to Interleukin-3

Mast cells are derived from HSCs via bipotent basophil/mast cell progenitors (BMCPs) and mast cell progenitors (MCPs) (Arinobu et al., 2005; Chen et al., 2005). Consistent with the increase in mast cells in the skin and gastrointestinal tract (data not shown), the numbers of BMCPs in spleen and MCPs in bone marrow were increased in young (6- to 10-week-old) *Plcb3*$^{-/-}$ mice (Figure S3A). Consistent with these in vivo results, 10-fold or more mast cells were generated from bone marrow cells of *Plcb3*$^{-/-}$ mice in interleukin (IL)-3-containing medium, compared to WT cells (Figure 3A), although expression levels of FcεRI and c-Kit were similar in both BMMCs (Figure 3B). IL-3-induced proliferation was 2- to 3-fold higher in *Plcb3*$^{-/-}$ than in WT BMMCs (Figure 3C), whereas stem cell factor (SCF)-induced proliferation was similar in the two genotypes. *Plcb3*$^{-/-}$ BMMCs migrated more vigorously toward IL-3 than WT cells (Figure 3D). On the other hand, growth factor withdrawal induced similar rates of apoptotic cell death in WT and *Plcb3*$^{-/-}$ BMMCs (data not shown). These results suggest that the increased proliferation and chemotaxis in response to IL-3 could be the major mechanisms for the increased mast cells in *Plcb3*$^{-/-}$ mice. This IL-3 hyperresponsiveness seems due to increased IL-3 receptor (IL-3R) signaling downstream of the receptor, given that expression of IL-3R in mast cells and that of IL-3 mRNA in skin tissues were comparable between WT and *Plcb3*$^{-/-}$ mice (Figures S3B and S3C).

PLC-β3 Inhibits Stat5 Activity in Mast Cells by Interacting with SHP-1 and Stat5

PLC-β3 interacts with Stat5 and SHP-1 to form the multimolecular SPS complex, and juxtaposition of SHP-1 and Stat5 via interactions with PLC-β3 enhances the catalytic activity of SHP-1 to dephosphorylate Stat5 (Xiao et al., 2009; Yasudo et al., 2011). As shown for *Plcb3*$^{-/-}$ HSCs (Xiao et al., 2009), IL-3-induced phosphorylation of Stat5 at Tyr^{694}, the phosphorylation site critical for its activation (Gouilleux et al., 1994), was enhanced in *Plcb3*$^{-/-}$ BMMCs (Figure 3E). Furthermore, phosphorylation of SHP-1 at Tyr^{536}, which is necessary for efficient interaction with Stat5 (Xiao et al., 2010), was abolished in *Plcb3*$^{-/-}$ cells.

Introduction of dominant-negative Stat5 drastically inhibited proliferation of *Plcb3*$^{-/-}$ BMMCs (Figure 3F). Transduction with WT SHP-1 restored SHP-1 phosphorylation and inhibited IL-3-induced Stat5 phosphorylation (Figure 3G) and mast cell proliferation (Figure 3F). These results show that IL-3 hyperresponsiveness caused by PLC-β3 deficiency depends on increased Stat5 activity and reduced SHP-1 activity. Given the comparable expression of IL-3 and IL-3R between WT and

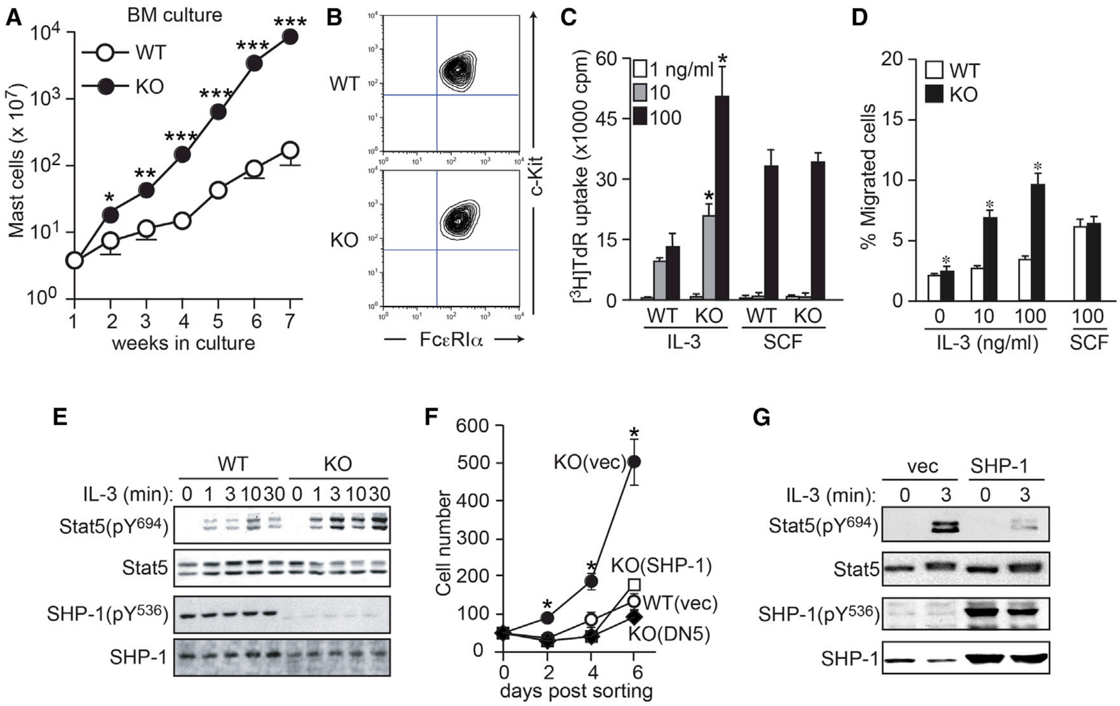

Figure 3. ***Plcb3*$^{-/-}$ Mast Cells Are Hypersensitive to IL-3 Stimulation**

(A) Bone marrow cells derived from WT or *Plcb3*$^{-/-}$ mice were cultured in IL-3-containing medium for the indicated periods. Live cells were counted.

(B) Greater than 98% of 5 week cultured BMMCs expressed c-Kit and FcεRI. Results in (A) and (B) are representative of at least ten experiments using three to four mice per group.

(C) BMMCs were depleted of IL-3 for 8 hr and cultured in the indicated concentrations of IL-3 or SCF for 36 hr. DNA synthesis was measured by [^{3}H]thymidine incorporation during the last 18 hr of culture.

(D) Chemotaxis of BMMCs toward IL-3 or SCF was assayed in Transwell for 8 hr. Results in (C) and (D) are representative of two experiments using three mice per group.

(E) WT and *Plcb3*$^{-/-}$ BMMCs were stimulated with 10 ng/ml of IL-3 for the indicated periods. Cell lysates were analyzed by SDS-PAGE followed by western blotting using antibodies for the indicated molecules.

(F and G) WT and *Plcb3*$^{-/-}$ MCPs were transduced with bicistronic retroviral vectors coding for DN Stat5 (DN5), WT SHP-1, or empty vector. GFP$^+$-transduced cells were FACS-sorted and cultured in IL-3 (F). *$p < 0.05$ versus empty vector-transduced WT cells (WT [vec]) by Student's t test. Some transduced *Plcb3*$^{-/-}$ mast cells were stimulated with IL-3 and subjected to western blot analysis (G).

Results in (E)–(G) are representative of two transduction experiments. In (A), (C), (D), and (F), data represent mean ± SEM. See also Figure S3.

Plcb3$^{-/-}$ mice (Figures S3B and S3C), not only IL-3 but also other factors that lead to Stat5 activation would contribute to the increased mast cells in *Plcb3*$^{-/-}$ mice.

Stat5 in Mast Cells Is Critical for Full Expression of Allergen-Induced Dermatitis

The above results imply that Stat5 and SHP-1 might contribute to dermatitis development by regulating the mast cell responsiveness to IL-3 (and other stimuli). To investigate this possibility more directly, we generated mice with mast cell-specific deletion of *Stat5* (*A* and *B*) or *Shp1* loci, termed *MCΔStat5* and *MCΔSHP-1* mice, respectively. Loss of expression of the targeted loci was confirmed by immunoblotting of neonatal skin-derived mast cells (Figure 4A) and/or immunofluorescence microscopy of skin mast cells (Figure S4A). Expression of Cre recombinase driven by the *Mcpt5* promoter (Scholten et al., 2008) did not affect numbers and distributions of T cells, B cells, or granulocytes (data not shown). Der f/SEB treatment induced significantly lower skin scores in *MCΔStat5* mice (Figure 4B) with lower infiltration of neutrophils and eosinophils (Figure 4D), but with WT levels of skin thickness (Figure 4C), compared to control mice. By contrast, higher skin scores were observed in *MCΔSHP-1* mice than in control mice (Figure S4B). There were similar numbers of mast cells in the ears of WT, *MCΔStat5* (Figure 4D), and *MCΔSHP-1* mice (Figure S4C). Mast cells reactive with phospho-Stat5 antibody were abundant in the inflammatory dermis from Der f/SEB-induced dermatitis (Figures 4E and 4F), although phospho-Stat5 positive cells were not restricted to mast cells. Further confirming the role of Stat5 in skin inflammation, TG101348, an inhibitor of Jak2 kinase that activates Stat5 activity (Pardanani et al., 2011), ameliorated Der f/SEB-induced dermatitis with reduced skin thickness and reduced numbers of mast cells, neutrophils and eosinophils (Figures S4D–S4F). These results collectively demonstrate that Stat5 activity in mast cells is required for full expression of allergen-induced skin inflammation.

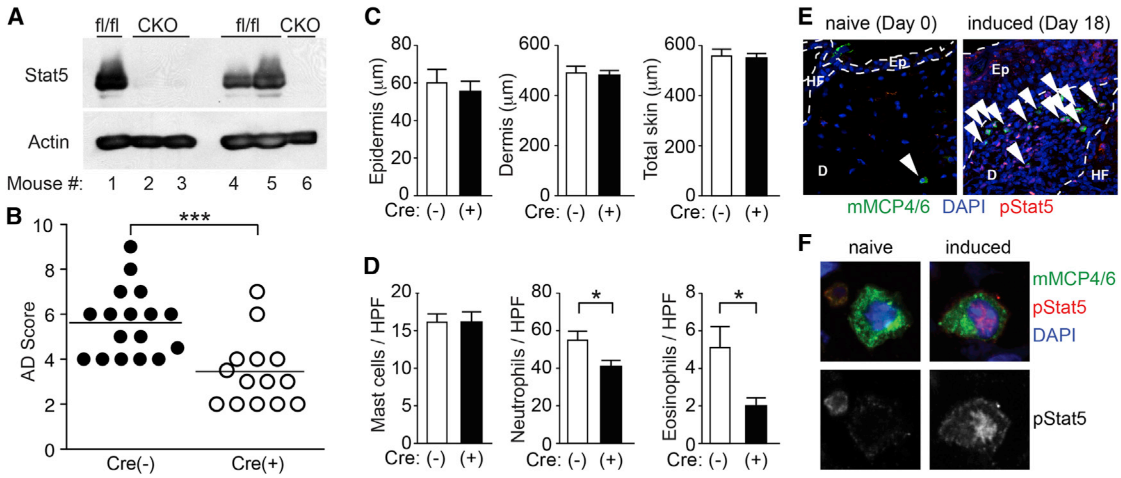

Figure 4. Stat5 in Mast Cells Regulates Der f/SEB-Induced Dermatitis

Dermatitis was induced with Der f/SEB in *MCΔStat5* mice [CKO or Cre(+)] and their floxed control [fl/fl or Cre(−)] mice. *$p < 0.05$, ***$p < 0.001$ by Student's t test.

(A) Western blot analysis of Stat5 in mast cells derived from neonatal skin of *MCΔStat5* (CKO) and control (fl/fl) mice.

(B) AD scores accumulated from four separate experiments using three to five mice per group.

(C) Thicknesses of epidermis and dermis after Der f/SEB (D/B) treatment.

(D) Histologic analysis of Der f/SEB-induced dermatitis. Data represent mean ± SEM.

(E and F) Skin sections of naive and Der f/SEB-induced (6 hr after fourth induction) dermatitis in WT mice were stained for phospho-Stat5, mMCP4, and mMCP6. Arrowheads indicate pStat5-positive mast cells. Ep, epidermis; D, dermis; HF, hair follicle. Representative images of mast cells from three experiments are shown in (E) and (F). See also Figure S4.

TSLP Is Highly Expressed in the Epidermis and Critical for Skin Inflammation in *Plcb3*$^{-/-}$ Mice

Overexpression of TSLP in keratinocytes in transgenic mice results in an AD-like phenotype (Li et al., 2005; Yoo et al., 2005). TSLP, which activates Stat5 (Isaksen et al., 1999), is highly expressed by keratinocytes in human AD (Soumelis et al., 2002) and, along with IL-1 and TNF, induces mast cells to secrete IL-13, IL-5, and other cytokines (Allakhverdi et al., 2007). TSLP expression is induced by various stimuli, including allergens, proteases, and mechanical injury (Ziegler, 2012). We next examined the role of TSLP in dermatitis in *Plcb3*$^{-/-}$ mice. Similar to a report (Bogiatzi et al., 2007), TSLP protein was highly expressed in the epidermis of lesional skin (Figure 5A), but *TSLP* mRNA levels were not increased in *Plcb3*$^{-/-}$ mice (data not shown). As expected, we observed TSLP expression in the epidermis in Der f/SEB-treated *Kit*$^{Wsh/W\text{-}sh}$ mice and identically treated WT mice. However, TSLP expression was more intense in the thickened epidermis in the latter mice than in the former mice (Figure S5A). It was even more exaggerated in Der f/SEB-treated *Plcb3*$^{-/-}$ and *Plcb3*$^{-/-}$*;Kit*$^{W\text{-}sh/W\text{-}sh}$ mice. We interpret that the overexpression of epidermal TSLP in *Plcb3*$^{-/-}$ and *Plcb3*$^{-/-}$*;Kit*$^{W\text{-}sh/W\text{-}sh}$ mice reflects the loss of PLC-β3-mediated suppression of TSLP expression in keratinocytes (Figure S5B) in these mice.

Importantly, no *Plcb3*$^{-/-}$*;TSLPR*$^{-/-}$ mice lacking both PLC-β3 and TSLPR (n = 10) developed dermatitis for 12 months (Figure 5B). Consistent with the role of TSLPR in Der f/SEB-induced dermatitis (Ando et al., 2013), Der f/SEB-induced dermatitis was less severe in *Plcb3*$^{-/-}$*;TSLPR*$^{-/-}$ mice than in *Plcb3*$^{-/-}$ mice (Figure 5C). Lesional skin in the former mice, which exhibited high levels of epidermal TSLP expression (data not shown), had reduced numbers of eosinophils and neutrophils (Figure 5D), but these mice had serum levels of IgE, similar to those of *Plcb3*$^{-/-}$ mice (data not shown). TSLP expression was low in Der f/SEB-treated skin of TG101348-treated mice (Figure S4G). Therefore, the TSLP-TSLPR axis is critically important for both spontaneous and allergen-induced dermatitis in *Plcb3*$^{-/-}$ mice.

Proinflammatory cytokines such as TNF, in combination with T_H2 cytokines, can induce the expression of TSLP in keratinocytes (Bogiatzi et al., 2007). However, all *Plcb3*$^{-/-}$*;TNF*$^{-/-}$ mice (n = 34) spontaneously developed dermatitis within 9 months (Figure 5E). Granulocyte macrophage colony stimulating factor (GM-CSF) can also activate Stat5 (Mui et al., 1995), promote T_H2 cell responses (Kusakabe et al., 2000), and might contribute to the establishment and chronicity of AD lesions (Bratton et al., 1995). Although GM-CSF contributed to epidermal and dermal thickening in allergen-induced skin inflammation (T.A. and T.K., unpublished data), all *Plcb3*$^{-/-}$*;GM-CSF*$^{-/-}$ mice (n = 31) spontaneously developed dermatitis within 8 months (Figure 5F). Therefore, both TNF and GM-CSF were dispensable for spontaneous skin inflammation in *Plcb3*$^{-/-}$ mice.

PLC-β3 Regulates Periostin Production by Fibroblasts

A recent study showed that periostin is a critical mediator for a Der f-induced AD model and that periostin expression is correlated with the severity of human AD (Masuoka et al., 2012). Periostin was highly expressed in the lesional dermis of spontaneous dermatitis in *Plcb3*$^{-/-}$ mice (Figure 6A) as well as Der f/SEB-induced dermatitis in WT and *Plcb3*$^{-/-}$ mice (Figure 6B). By contrast, its protein and mRNA expression was reduced in Der f/SEB-induced dermatitis in mast cell-deficient

Cell PRESS Open ACCESS

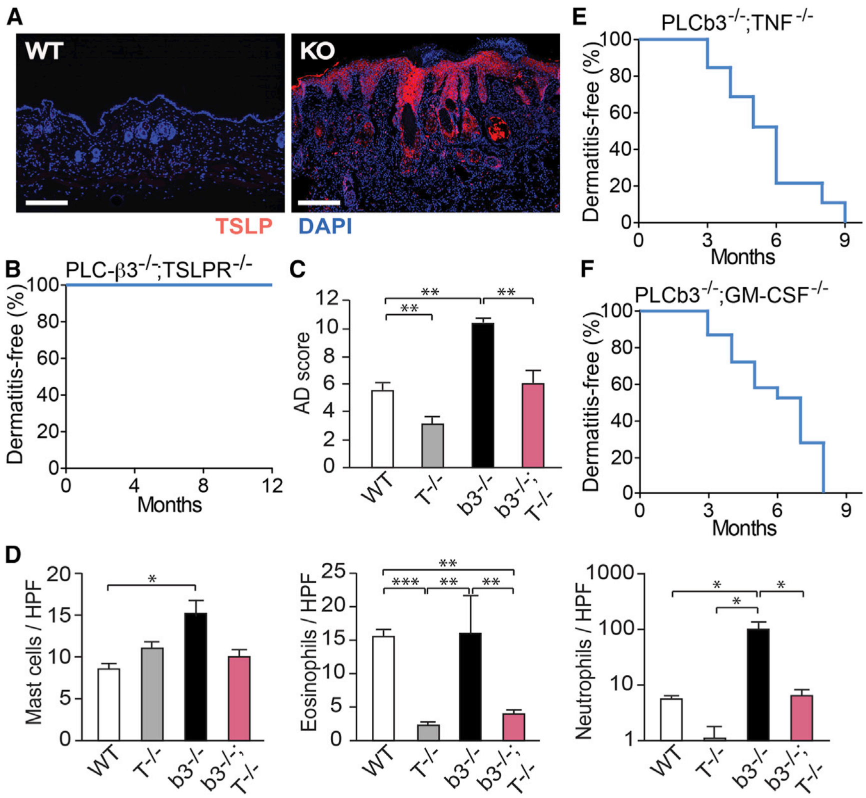

Figure 5. Role of the TSLP-TSLPR Axis in Der f/SEB-Induced Dermatitis and Spontaneous Dermatitis in *Plcb3*$^{-/-}$ Mice

(A) Lesional skin from 10-month-old *Plcb3*$^{-/-}$ mice and healthy control (WT) were stained for TSLP (red) and nuclei (blue).

(B) Kaplan-Meier plots for dermatitis development in *Plcb3*$^{-/-}$;*TSLPR*$^{-/-}$ (n = 10).

(C) Dermatitis was induced with Der f/SEB in WT, *TSLPR*$^{-/-}$ (T$^{-/-}$), *Plcb3*$^{-/-}$ (b3$^{-/-}$), and *Plcb3*$^{-/-}$;*TSLPR*$^{-/-}$ (b3$^{-/-}$;T$^{-/-}$) mice.

(D) Histologic analysis of Der f/SEB-induced dermatitis. Data represent mean ± SEM.

(E and F) Kaplan-Meier plots for dermatitis development in *Plcb3*$^{-/-}$;*TNF*$^{-/-}$ (n = 34), and *Plcb3*$^{-/-}$;*GM-CSF*$^{-/-}$ (n = 31) mice.

Results in (C) and (D) are representative of two independent experiments using three to six mice per group. *$p < 0.05$, **$p < 0.01$, ***$p < 0.001$ by ANOVA. See also Figure S5.

mice (Figures 6B and 6C). Consistent with the known role of periostin in fibrosis, Masson trichrome staining confirmed remarkable fibrosis in skin lesions of spontaneous dermatitis (Figure S1C) and Der f/SEB-induced dermatitis (data not shown). To further analyze periostin expression, embryonic fibroblasts (MEFs) and NIH/3T3 fibroblasts were used. When fibroblasts were cocultured with IgE/antigen-stimulated BMMC, periostin secretion was increased (Figure 6D). We confirmed that IL-13, a major cytokine produced by IgE/antigen-stimulated mast cells (Burd et al., 1995), enhances the production and secretion of periostin in fibroblasts (Figure 6E). These results collectively demonstrate that mast cells can regulate periostin production in fibroblasts.

Importantly, basal levels of periostin were remarkably higher in *Plcb3*$^{-/-}$ than in WT MEFs. Therefore, constitutive expression of periostin appeared to be negatively regulated by PLC-β3. Costimulation of WT, but not *Plcb3*$^{-/-}$, MEFs with TSLP inhibited IL-13-induced periostin production/secretion (Figure 6F). This result suggests the presence of feedback inhibition in the skin for fibroblasts' periostin production by TSLP, which can be induced in keratinocytes by periostin (Masuoka et al., 2012), and this feedback inhibition is lost in *Plcb3*$^{-/-}$ MEFs. We also found that TSLP mRNA expression is higher in *Plcb3*$^{-/-}$ than in WT keratinocytes (Figure S5B), consistent with increased TSLP expression in the epidermis of lesional skin of *Plcb3*$^{-/-}$ mice (Figure 5A). These results not only add a cellular component (i.e., mast cells) to the hypothetical vicious cycle of skin inflammation consisting of T_H2 cytokines (from T_H2 cells)-periostin (from fibroblasts)-TSLP (from keratinocytes) (Masuoka et al., 2012), but also show that PLC-β3 intrinsically regulates periostin production in fibroblasts and TSLP expression in keratinocytes.

Association of the SPS Complex Genes and Mast Cell-Expressed Phospho-STAT5 with Human AD

The clinical relevance of Der f/SEB-induced dermatitis was supported by similarity in gene expression profiles between this dermatitis and human AD (Ando et al., 2013). Gene expression profiles in spontaneous dermatitis in *Plcb3*$^{-/-}$ mice were also more similar to those in human AD than those in human psoriasis (Table S1). In light of the strong clinical relevance of the two dermatitis models and functional relationship among PLC-β3, STAT5, and SHP-1 in mast cells, we genotyped single nucleotide polymorphisms (SNPs) for these genes (Table S2) in AD populations (Table S3). The AD patients were stratified as ADEH^{+} and ADEH^{-} based on those who suffered eczema herpeticum and those who did not, respectively. Eczema herpeticum is a severe disseminated herpes virus infection that occurs at skin lesions of AD and other conditions (Wollenberg et al., 2003); ADEH^{+} patients suffer more severe dermatitis than ADEH^{-} patients (Beck et al., 2009). Among the *PLCB3* SNPs tested, rs2244625 was associated with risk of ADEH in European American subjects (Table S4). Furthermore, a nonsynonymous SNP (rs35169799) was significantly associated with decreased levels of IgE among controls but not among AD subjects (Figure S6A). Table S4 shows that *STAT5B* SNP rs9900213 and *SHP1* SNP rs7310161 were significantly associated with the risk of AD among European American subjects. One *STAT5A* SNP (rs16967637) and four *SHP1* SNPs were associated with the severity of AD among African Americans. No AD-associated SNPs except for rs35169799 change protein structures.

Finally, we found that mast cells are more abundant in the dermis of AD lesions than in that of nonlesional skin of AD patients or healthy individuals (Figures 7A and 7B). More importantly, mast cells were abundantly detected with higher

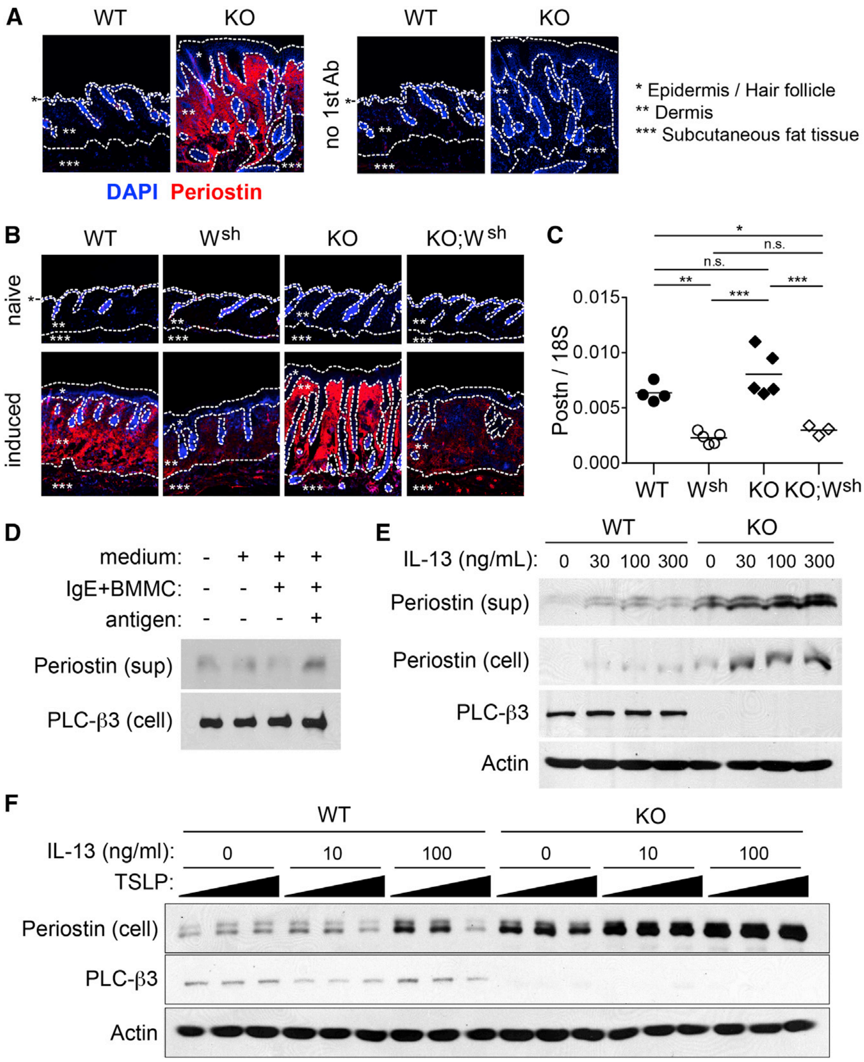

Figure 6. Regulation of Periostin Production in Fibroblasts

(A) Lesional skin of spontaneous dermatitis in *Plcb3*$^{-/-}$ mice (KO) and normal skin from WT mice (WT) were stained for periostin (red) and nuclei (blue). Right panels show control stainings without antiperiostin antibody.

(B) Periostin was stained before (naive) and after Der f/SEB induction of dermatitis (induced) in WT, *Kit*$^{W\text{-}sh/W\text{-}sh}$ (Wsh), *Plcb3*$^{-/-}$ (KO), and *Plcb3*$^{-/-}$;*Kit*$^{W\text{-}sh/W\text{-}sh}$ (KO;W^{sh}) mice. Borders of epidermis, dermis and subcutaneous fat tissues are indicated by dotted lines.

(C) Periostin mRNA expression in Der f/SEB-treated skin was quantified by qPCR.

(D) NIH/3T3 cells were incubated with or without IgE-sensitized BMMCs in the presence or absence of antigen.

(E and F) WT and *Plcb3*$^{-/-}$ MEFs were stimulated by the indicated concentrations of IL-13 in the absence (E) or presence (F) of 0, 10, or 100 ng/ml of TSLP for 24 hr.

Results in (A)–(C) are representative of three experiments using three to five mice per group. Periostin protein in culture supernatants and lysates of the cells was analyzed by western blotting. $^{*}p < 0.05$, $^{**}p < 0.01$, $^{***}p < 0.001$ by ANOVA. In vitro experiments with results similar to (D)–(F) were performed two to four times. See also Figure S7.

nuclear intensities of phospho-STAT5 staining in lesional skin of some AD patients (Figures 7C–7E). Nuclear STAT5 phosphorylation in mast cells was correlated with skin mast cell numbers (Figure S6B) and inversely correlated with PLC-β3 expression in mast cells (Figures S6C–S6F). The above SNP and immunofluorescence data support the idea that dysregulation of the SPS complex leading to STAT5 activation is involved at least in some cases of human AD.

DISCUSSION

In this study, we showed that mast cells, but not αβ T or B cells, are required for spontaneously occurring dermatitis in *Plcb3*$^{-/-}$ mice. We show a mast cell-dependent naturally occurring AD model (Kawakami et al., 2009), despite the limitations of Kit mutant mice as a model of mast cell deficiency (Rodewald and Feyerabend, 2012). *Plcb3*$^{-/-}$ mast cells were hyperresponsive to IL-3 due to increased Stat5 activity, which could be antagonized by PLC-β3 and SHP-1. These in vitro results support the in vivo anti-inflammatory role of PLC-β3 and SHP-1 that regulate the proliferative and chemotactic behavior of mast cells by controlling Stat5 activity. Characterization of spontaneous dermatitis in *Plcb3*$^{-/-}$ mice was complemented by allergen-induced dermatitis experiments, as the particular importance of Stat5 regulation in mast cells was demonstrated by alleviated allergen-induced dermatitis in mice lacking Stat5 in mast cells and by efficient suppression of allergen-induced dermatitis by chemical inhibition of Stat5 activity. Spontaneous dermatitis in *Plcb3*$^{-/-}$ mice depended on the TSLP/TSLPR axis, which uses Stat5 as a critical signal transducer (Isaksen et al., 1999). Thus, Stat5 activation is required for the development of both spontaneous and allergen-induced dermatitis. Human data suggest that STAT5 activating pathways in mast cells are operational in a subset of AD patients.

Various studies suggest the role of T cells in AD pathogenesis (Jin et al., 2009a; Kawakami et al., 2009). Skin inflammation in our Der f/SEB model requires αβ T cells (Ando et al., 2013), in line with the widely accepted scenario for AD development (Bieber, 2008; Boguniewicz and Leung, 2011): impaired skin barrier function allows allergens easy access to the inside of skin; allergens are taken up by Langerhans cells and dermal dendritic cells, and these cells migrate and mature to present allergens to naive helper T cells in lymph nodes; activated and differentiated T_H2 cells migrate back to skin sites re-exposed to allergens; these effector T_H2 cells recruit mast cells, eosinophils, and other granulocytes in order to cause tissue damages.

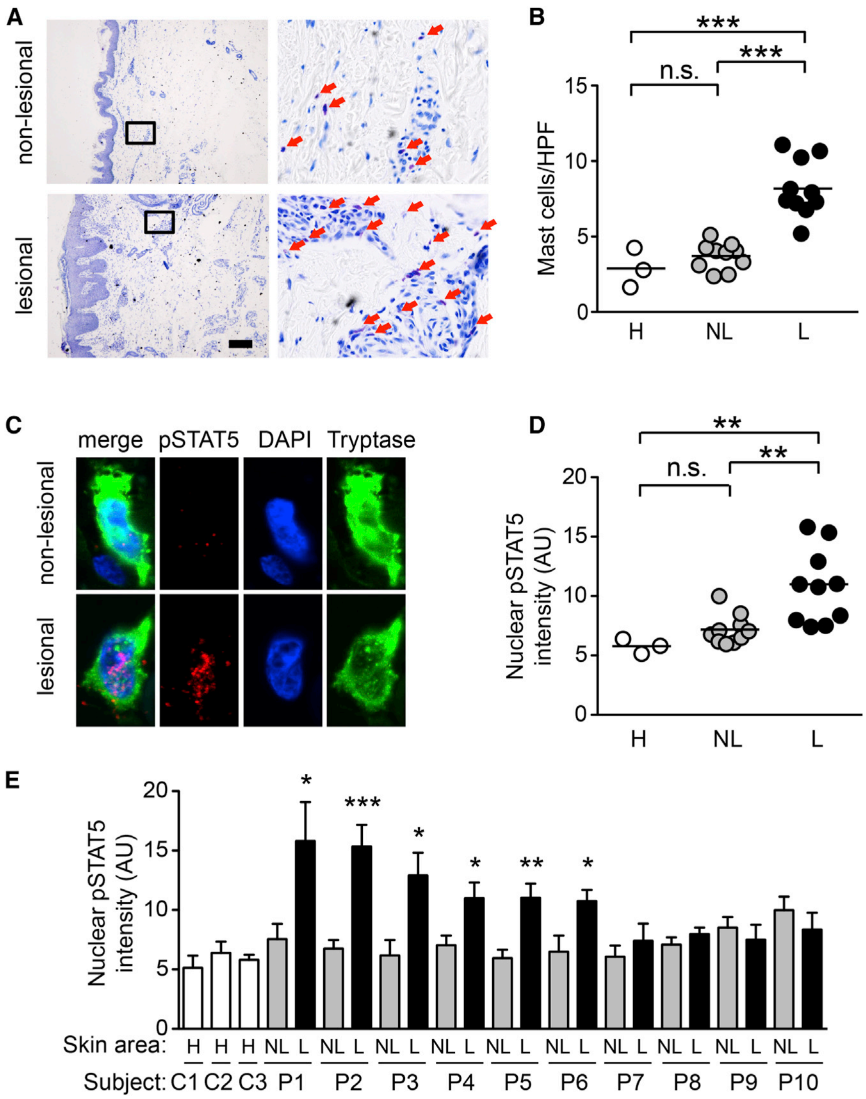

Figure 7. Increased Numbers of Mast Cells with Enhanced STAT5 Phosphorylation in Human AD Patients

(A) Lesional and nonlesional skin samples of human AD patients were analyzed by Toluidine blue staining. Portions indicated by rectangle are enlarged on right panels. Red arrows indicate mast cells.

(B) Quantification of mast cells. **p < 0.01; ***p < 0.001 by Tukey's multiple comparison test (ANOVA).

(C) Skin samples of human AD patients were stained for phospho-STAT5 (red), tryptase (green), and nuclei (blue). Representative images are shown from patient P1.

(D and E) Nuclear phospho-STAT5 levels in mast cells in lesional (L) and nonlesional (NL) skin samples of human AD patients and healthy skin (H) were measured by ImageJ software (NIH). Data represent mean ± SEM. *p < 0.05, **p < 0.01, ***p < 0.001 versus nonlesional (NL) skin by Student's t test. See also Figure S6 and Tables S1–S4.

Although αβ T cells were dispensable for spontaneous dermatitis in *Plcb3*$^{-/-}$ mice, αβ T cells seem to contribute to a severe phenotype in this dermatitis. Thus, skin inflammation in *Plcb3*$^{-/-}$;*TCRβ*$^{-/-}$ mice was less prominent than that in *Plcb3*$^{-/-}$ mice (data not shown). By contrast, B cells (the source of IgE) appeared to be dispensable for both spontaneous dermatitis and allergen-induced dermatitis, although there was a clear correlation between IgE levels and the severity of dermatitis. This apparent discrepancy seems to be related to the presence of both activating (FcεRI) and inhibitory (FcγRIIb) receptors for IgE in mast cells (and other cells), given that FcεRI was required for maximal allergen-induced skin inflammation.

Masuoka et al. (2012) recently proposed a vicious cycle for allergic skin inflammation consisting of T_H2 cytokines (from T_H2 cells)-periostin (from fibroblasts)-TSLP and other proinflammatory cytokines (from keratinocytes). Our Der f/SEB induction model requires T cells for full-blown dermatitis, whereas spontaneous and persistent dermatitis in *Plcb3*$^{-/-}$ mice does not. The TSLP-TSLPR axis and mast cells are required for both AD models (this study; Ando et al., 2013), whereas T cells are required only for allergen-induced dermatitis. Therefore, we speculate that T cells and mast cells are required for TSLP overexpression. Once sustained overexpression of TSLP is established, mast cells may play a more important role in persistent dermatitis as the cellular source of T_H2 cytokines (Figure S7). Related to this network, our current study showed that PLC-β3 can regulate activities of the cellular elements of the network, such as proliferation in mast cells, periostin expression in fibroblasts and TSLP expression in keratinocytes. Our data also suggest the presence of a feedback loop for inhibition of fibroblasts' periostin production by TSLP, and PLC-β3 in fibroblasts is required for this negative feedback. Among the cytokines induced in keratinocytes by periostin, we found that TSLP, but not TNF or GM-CSF, is important for the development of spontaneous dermatitis in *PLC-β3*$^{-/-}$ mice.

Our human data are consistent with mouse data by showing genetic linkage with all four genes that encode components of the SPS complex. Although IL-3 alone or IL-3 plus IL-4 cannot induce the differentiation of human mast cells (Saito et al., 1988), human mast cells express functional receptors for IL-3, IL-5, and GM-CSF (Dahl et al., 2004), and, along with SCF, IL-3 can enhance mast cell growth by decreasing mast cell apoptosis (Gebhardt et al., 2002). Interestingly, silencing of STAT5A and STAT5B expression induced apoptosis in human mast cells (J.K. and T.K., unpublished data). Thus, the breakdown of PLC-β3/SHP-1-dependent suppression of STAT5 activity, which is recruited by IL-3 or other cytokines in human mast cells, may represent a pathogenic mechanism for human AD. Alternatively, SPS complexes might regulate the growth properties of cell types other than mast cells. Several cytokines including IL-5, IL-21, IL-31, TSLP, and GM-CSF, which are implicated in AD pathogenesis (Jin et al., 2009b; Sonkoly et al., 2006; Soumelis et al., 2002; Yamamoto et al., 2003), utilize the JAK-STAT5 pathway for their signal transduction. Reduced expression of PLC-β3, thus improper regulation of STAT5 activity in those cells, would contribute to AD development. These considerations provide additional reasoning for the JAK-STAT5 pathway as a potential target of AD treatment. However, not all AD patients showed increased expression of STAT5 phosphorylation in mast cells. Thus, stratification of AD by STAT5 phosphorylation and/or PLC-β3 expression may be important for clinical application of our results.

EXPERIMENTAL PROCEDURES

Human Subjects

Two independent populations were used for genetic association analysis, including 414 European American subjects and 323 African American subjects. Subjects were recruited as part of the NIAID-supported Atopic Dermatitis and Vaccinia Network (ADVN). Demographic characteristics are presented in Table S3. AD patients and healthy individuals were also recruited at University of California San Diego. Skin biopsies using a 4 mm punch biopsy were performed on a lesional target site of atopic skin and a target nonlesional site at least 4 cm from the lesional site. Normal matched control samples were obtained from healthy donors in similar locations.

AD Diagnosis and Phenotypes

AD was diagnosed using the US consensus conference criteria (Eichenfield et al., 2003). ADEH was defined as AD patients with at least one eczema herpeticum episode documented either by an ADVN investigator or by another physician confirmed by PCR detection of HSV infection, tissue immunofluorescence, Tzanck smear, and/or culture. AD severity was defined according to the "eczema area and severity index" (EASI), a standardized grading system (Hanifin et al., 2001), and total serum IgE was measured using the UniCap 250 system (Pharmacia and Upjohn). Clinical characteristics are presented in Table S3. The study was approved by the institutional review boards at National Jewish Health in Denver, Johns Hopkins University, Oregon Health and Science University, University of California San Diego, Children's Hospital of Boston, and University of Rochester. All subjects gave written informed consent prior to participation.

Genotyping and Quality Control

A total of 22 SNPs for the four candidate genes were selected from the HapMap (http://www.hapmap.org/) using a tagging approach: eight *PLCb3* SNPs, six *STAT5A* SNPs, four *STAT5B* SNPs, and four *SHP1* SNPs. The four SNPs in *STAT5B* were genotyped using the custom-designed Illumina OPA for the BeadXpress Reader System and the GoldenGate Assay with VeraCode Bead technology according to the manufacturer's protocol. The rest of SNPs were genotyped and analyzed on a 7900HT Sequence Detection System (Applied Biosystems) with Applied Biosystems Genotyper software (SDS system, version 2.2). As part of quality control, we genotyped additional 74 SNPs identified as ancestry informative markers selected for maximal difference between African and European populations and assessed potential confounding factors due to population substructure using genotype data and the STRUCTURE program (v.2.2; http://pritch.bsd.uchicago.edu/software).

Mice

Plcb3$^{-/-}$ mice were backcrossed to C57BL/6 mice for 12 generations. C57BL/6-*Kit*$^{W\text{-}sh/W\text{-}sh}$ mice were bred to *Plcb3*$^{-/-}$ mice, and their F1 mice were intercrossed to generate mast cell-deficient *Kit*$^{W\text{-}sh/W\text{-}sh}$;*Plcb3*$^{-/-}$ mice. Other double-mutant mice were similarly generated. Dermatitis in both male and female mice under SPF conditions was scored by gross appearance and confirmed by histology. Animal experiments were approved by the Animal Use and Care Committee of the La Jolla Institute for Allergy and Immunology (LIAI) and carried out in the LIAI animal facility.

Mast Cell Engraftment

BMMCs derived from female *Plcb3*$^{-/-}$ mice were transferred by intradermal injection (4×10^6 cells in 50 μl DMEM per site, totally 20 sites distributed in five rows down the length of shaved back skin) into 4-week-old female *Plcb3*$^{-/-}$;*Kit*$^{W\text{-}sh/W\text{-}sh}$ mice.

Der f/SEB Induction of AD-like Skin Lesions

AD-like skin lesions were induced by two rounds of epicutaneous treatment of shaved back skin of male mice with Der f and SEB as described (Kawakami et al., 2007). AD scores are based on the severity (0, no symptoms; 1, mild; 2, intermediate; 3, severe) of four possible symptoms (redness, bleeding, eruption, and scaling). A scientist who did not know the identities of mice scored skin lesions.

Cultures of Mast Cells and Retroviral Transduction

Bone marrow cells or MCPs purified by fluorescence-activated cell sorting (FACS) (Chen et al., 2005) were cultured in IL-3-containing medium. Live cells were counted during weekly media changes. Recombinant retroviruses were generated by transfection of Plat-E cells with pMIG vectors. Bone marrow cells or MCPs were infected with the retroviruses, and GFP^+ cells were FACS purified and cultured.

Neonatal Skin-Derived Mast Cells

Newborn skin was incubated with 0.5% trypsin-EDTA (Invitrogen) for 1 hr, and epidermis was removed. Separated dermis was minced and incubated in DMEM containing 2 U/mL of Liberase TL (Roche Applied Science) and 1.6 mg/ml of hyaluronidase (Sigma-Aldrich). Dispersed cells were cultured in RPMI1640 supplemented with 10% FCS, IL-3, and SCF. $Fc\varepsilon RI\alpha^+$ c-Kit^+ cells were sorted and subject to immunoblot analysis.

Microarray Analysis of Gene Expression

RNA preparation, microarrays, and data analysis were described previously (Ando et al., 2013). Data have been deposited in the NCBI Gene Expression Omnibus under accession number GSE53132.

Histology

Skin biopsies were fixed with 10% formaldehyde and embedded in paraffin. Sections were stained with hematoxylin and eosin staining (H&E), Toluidine blue, Congo-red, or Masson trichrome. For immunohistochemistry, skin biopsies were immediately embedded in O.C.T. compound (Sakura Tissue-Tek) and stored at −80°C. Cryosections were fixed, and endogenous peroxidase was quenched with 3% H_2O_2 in cold methanol. ABC Staining Systems (Santa Cruz Biotechnology) were used to visualize stainings with anti-CD4 (Santa Cruz), anti-CD8 (BD Biosciences), or anti-Mac-1 (BD Biosciences) as primary antibodies. For immunofluorescence, biopsies were fixed in 4% paraformaldehyde at 4°C, washed in 10%–20% sucrose in phosphate buffered saline, embedded in O.C.T. compound, and stored at −80°C. Cryosections were dried, rehydrated, and incubated with anti-CD4, anti-CD8, anti-F4/80 (Abcam), or anti-TSLP (Amgen) at 4°C overnight. After washing, sections were incubated with Texas-red-conjugated goat anti-rat IgG (Southern Biotech), and mounted with ProLong Gold antifade reagent with DAPI (Invitrogen). For the detection of periostin and phospho-Stat5 in mast cells, 10% formalin-fixed sections were subjected to heat-induced antigen retrieval after deparaffinization. Antiperiostin (Masuoka et al., 2012), anti-phospho-Stat5 (Abcam), anti-mast cell tryptase (Abcam), or anti-mMCP4 and anti-mMCP6 (Shin et al., 2006) was used as a primary antibody, in combination with Alexa-Fluor-488-, -568-, or -647-conjugated goat anti-mouse, anti-rat, or anti-rabbit antibody (Invitrogen) as a secondary antibody. Fluorescent images were observed at the magnification of 400 under either Nikon Eclipse 80i fluorescence microscope or Olympus FluoView FV10i confocal laser microscope. Human skin mast cells were counted (>100 per sample) in rectangular regions covering the entire skin layers from the epidermis to subcutaneous adipose tissues.

Flow cytometry

Expression of c-Kit, FcεRI, and IL-3 receptor on mast cells was analyzed using FACSCalibur (BD Biosciences) after staining with APC-conjugated anti-c-Kit (2B8, BD Biosciences), FITC-conjugated anti-FcεRI (MAR-1, BioLegend), or PE-conjugated anti-iL-3 receptor (5B11, BD Biosciences).

Immunoblotting

Mast cells were stimulated with IL-3 and lysed in 1% NP-40 lysis buffer. Lysates were analyzed by SDS-PAGE followed by electroblotting to PVDF membranes (Millipore). Membranes were incubated with a primary antibody and then with an HRP-conjugated secondary antibody. Antibody-bound proteins were revealed by ECL reagent (PerkinElmer).

Statistical Analysis

For genetic analysis, logistic regression, adjusting for the first two principal components, was used to test for association between each individual marker (under an additive model) and disease status using PLINK software (http://pngu.mgh.harford.edu/~purcell/plink/to). To test for association between genetic markers and total serum levels of log-adjusted IgE and log-adjusted EASI score, we used linear regression models adjusting for confounding variables age and gender as well as the first two principal components. Departures from Hardy-Weinberg equilibrium at each locus were tested with chi-square tests separately for cases and controls using PLINK. Other statistical analyses are performed by Student's t test, ANOVA, or Tukey's test as shown.

ACCESSION NUMBERS

Microarray data have been deposited in the NCBI Gene Expression Omnibus under accession number GSE53132.

SUPPLEMENTAL INFORMATION

Supplemental Information includes Supplemental Experimental Procedures, seven figures, and four tables and can be found with this article online at http://dx.doi.org/10.1016/j.celrep.2013.12.029.

ACKNOWLEDGMENTS

We thank other ADVN members for allowing us to use the DNAs collected through the network. The ADVN was supported by the National Institute of Allergy and Infectious Diseases/NIH (N01 AI40030). We are thankful to Drs. Lothar Hennighausen, Klaus Rajewsky, and Steven F. Ziegler for donating mice. M.K. participated in this study as a graduate student in the Department of Rheumatology and Infectious Diseases, Kitasato University School of Medicine. This study was in part supported by contract and grants from the NIH (HHSN26620040033C), MPN Foundation, and Ministry of Education, Culture, Sports, Science and Technology of Japan. W.X. was supported in part by the Diabetes and Immune Disease National Research Institute, J.-i.K. was supported in part by the Takeda Science Foundation, and K.C.B. was supported in part by the Mary Beryl Patch Turnbull Scholar Program. This manuscript is Publication 1148 from the La Jolla Institute for Allergy and Immunology.

Received: March 28, 2013
Revised: October 21, 2013
Accepted: December 17, 2013
Published: January 9, 2014

REFERENCES

Allakhverdi, Z., Comeau, M.R., Jessup, H.K., Yoon, B.R., Brewer, A., Chartier, S., Paquette, N., Ziegler, S.F., Sarfati, M., and Delespesse, G. (2007). Thymic stromal lymphopoietin is released by human epithelial cells in response to microbes, trauma, or inflammation and potently activates mast cells. J. Exp. Med. *204*, 253–258.

Ando, T., Matsumoto, K., Namiranian, S., Yamashita, H., Glatthorn, H., Kimura, M., Dolan, B.R., Lee, J.J., Galli, S.J., Kawakami, Y., et al. (2013). Mast cells are required for full expression of allergen/SEB-induced skin inflammation. J. Invest. Dermatol. *133*, 2695–2705.

Arinobu, Y., Iwasaki, H., Gurish, M.F., Mizuno, S., Shigematsu, H., Ozawa, H., Tenen, D.G., Austen, K.F., and Akashi, K. (2005). Developmental checkpoints of the basophil/mast cell lineages in adult murine hematopoiesis. Proc. Natl. Acad. Sci. USA *102*, 18105–18110.

Beck, L.A., Boguniewicz, M., Hata, T., Schneider, L.C., Hanifin, J., Gallo, R., Paller, A.S., Lieff, S., Reese, J., Zaccaro, D., et al. (2009). Phenotype of atopic dermatitis subjects with a history of eczema herpeticum. J. Allergy Clin. Immunol. *124*, 260–269, e1–e7.

Bieber, T. (2008). Atopic dermatitis. N. Engl. J. Med. *358*, 1483–1494.

Bogiatzi, S.I., Fernandez, I., Bichet, J.C., Marloie-Provost, M.A., Volpe, E., Sastre, X., and Soumelis, V. (2007). Cutting Edge: Proinflammatory and Th2 cytokines synergize to induce thymic stromal lymphopoietin production by human skin keratinocytes. J. Immunol. *178*, 3373–3377.

Boguniewicz, M., and Leung, D.Y. (2011). Atopic dermatitis: a disease of altered skin barrier and immune dysregulation. Immunol. Rev. *242*, 233–246.

Bratton, D.L., Hamid, Q., Boguniewicz, M., Doherty, D.E., Kailey, J.M., and Leung, D.Y. (1995). Granulocyte macrophage colony-stimulating factor contributes to enhanced monocyte survival in chronic atopic dermatitis. J. Clin. Invest. *95*, 211–218.

Burd, P.R., Thompson, W.C., Max, E.E., and Mills, F.C. (1995). Activated mast cells produce interleukin 13. J. Exp. Med. *181*, 1373–1380.

Chen, C.C., Grimbaldeston, M.A., Tsai, M., Weissman, I.L., and Galli, S.J. (2005). Identification of mast cell progenitors in adult mice. Proc. Natl. Acad. Sci. USA *102*, 11408–11413.

Dahl, C., Hoffmann, H.J., Saito, H., and Schiøtz, P.O. (2004). Human mast cells express receptors for IL-3, IL-5 and GM-CSF; a partial map of receptors on human mast cells cultured in vitro. Allergy *59*, 1087–1096.

Eichenfield, L.F., Hanifin, J.M., Luger, T.A., Stevens, S.R., and Pride, H.B. (2003). Consensus conference on pediatric atopic dermatitis. J. Am. Acad. Dermatol. *49*, 1088–1095.

Gebhardt, T., Sellge, G., Lorentz, A., Raab, R., Manns, M.P., and Bischoff, S.C. (2002). Cultured human intestinal mast cells express functional IL-3 receptors and respond to IL-3 by enhancing growth and IgE receptor-dependent mediator release. Eur. J. Immunol. *32*, 2308–2316.

Gouilleux, F., Wakao, H., Mundt, M., and Groner, B. (1994). Prolactin induces phosphorylation of Tyr694 of Stat5 (MGF), a prerequisite for DNA binding and induction of transcription. EMBO J. *13*, 4361–4369.

Hamilton, D.W. (2008). Functional role of periostin in development and wound repair: implications for connective tissue disease. J. Cell Commun. Signal. *2*, 9–17.

Hanifin, J.M., Thurston, M., Omoto, M., Cherill, R., Tofte, S.J., and Graeber, M.; EASI Evaluator Group (2001). The eczema area and severity index (EASI): assessment of reliability in atopic dermatitis. Exp. Dermatol. *10*, 11–18.

Isaksen, D.E., Baumann, H., Trobridge, P.A., Farr, A.G., Levin, S.D., and Ziegler, S.F. (1999). Requirement for stat5 in thymic stromal lymphopoietin-mediated signal transduction. J. Immunol. *163*, 5971–5977.

Jin, H., He, R., Oyoshi, M., and Geha, R.S. (2009a). Animal models of atopic dermatitis. J. Invest. Dermatol. *129*, 31–40.

Jin, H., Oyoshi, M.K., Le, Y., Bianchi, T., Koduru, S., Mathias, C.B., Kumar, L., Le Bras, S., Young, D., Collins, M., et al. (2009b). IL-21R is essential for epicutaneous sensitization and allergic skin inflammation in humans and mice. J. Clin. Invest. *119*, 47–60.

Kawakami, Y., Yumoto, K., and Kawakami, T. (2007). An improved mouse model of atopic dermatitis and suppression of skin lesions by an inhibitor of Tec family kinases. Allergol. Int. *56*, 403–409.

Kawakami, T., Ando, T., Kimura, M., Wilson, B.S., and Kawakami, Y. (2009). Mast cells in atopic dermatitis. Curr. Opin. Immunol. *21*, 666–678.

Kusakabe, K., Xin, K.Q., Katoh, H., Sumino, K., Hagiwara, E., Kawamoto, S., Okuda, K., Miyagi, Y., Aoki, I., Nishioka, K., et al. (2000). The timing of GM-CSF expression plasmid administration influences the Th1/Th2 response induced by an HIV-1-specific DNA vaccine. J. Immunol. *164*, 3102–3111.

Li, M., Messaddeq, N., Teletin, M., Pasquali, J.L., Metzger, D., and Chambon, P. (2005). Retinoid X receptor ablation in adult mouse keratinocytes generates an atopic dermatitis triggered by thymic stromal lymphopoietin. Proc. Natl. Acad. Sci. USA *102*, 14795–14800.

Liu, Y.J. (2006). Thymic stromal lymphopoietin: master switch for allergic inflammation. J. Exp. Med. *203*, 269–273.

Masuoka, M., Shiraishi, H., Ohta, S., Suzuki, S., Arima, K., Aoki, S., Toda, S., Inagaki, N., Kurihara, Y., Hayashida, S., et al. (2012). Periostin promotes chronic allergic inflammation in response to Th2 cytokines. J. Clin. Invest. *122*, 2590–2600.

Mui, A.L., Wakao, H., O'Farrell, A.M., Harada, N., and Miyajima, A. (1995). Interleukin-3, granulocyte-macrophage colony stimulating factor and interleukin-5 transduce signals through two STAT5 homologs. EMBO J. *14*, 1166–1175.

Pardanani, A., Gotlib, J.R., Jamieson, C., Cortes, J.E., Talpaz, M., Stone, R.M., Silverman, M.H., Gilliland, D.G., Shorr, J., and Tefferi, A. (2011). Safety and efficacy of TG101348, a selective JAK2 inhibitor, in myelofibrosis. J. Clin. Oncol. *29*, 789–796.

Rodewald, H.R., and Feyerabend, T.B. (2012). Widespread immunological functions of mast cells: fact or fiction? Immunity *37*, 13–24.

Ruan, K., Bao, S., and Ouyang, G. (2009). The multifaceted role of periostin in tumorigenesis. Cell. Mol. Life Sci. *66*, 2219–2230.

Saito, H., Hatake, K., Dvorak, A.M., Leiferman, K.M., Donnenberg, A.D., Arai, N., Ishizaka, K., and Ishizaka, T. (1988). Selective differentiation and proliferation of hematopoietic cells induced by recombinant human interleukins. Proc. Natl. Acad. Sci. USA *85*, 2288–2292.

Scholten, J., Hartmann, K., Gerbaulet, A., Krieg, T., Müller, W., Testa, G., and Roers, A. (2008). Mast cell-specific Cre/loxP-mediated recombination in vivo. Transgenic Res. *17*, 307–315.

Shin, K., Gurish, M.F., Friend, D.S., Pemberton, A.D., Thornton, E.M., Miller, H.R., and Lee, D.M. (2006). Lymphocyte-independent connective tissue mast cells populate murine synovium. Arthritis Rheum. *54*, 2863–2871.

Sonkoly, E., Muller, A., Lauerma, A.I., Pivarcsi, A., Soto, H., Kemeny, L., Alenius, H., Dieu-Nosjean, M.C., Meller, S., Rieker, J., et al. (2006). IL-31: a new link between T cells and pruritus in atopic skin inflammation. J. Allergy Clin. Immunol. *117*, 411–417.

Soumelis, V., Reche, P.A., Kanzler, H., Yuan, W., Edward, G., Homey, B., Gilliet, M., Ho, S., Antonenko, S., Lauerma, A., et al. (2002). Human epithelial cells trigger dendritic cell mediated allergic inflammation by producing TSLP. Nat. Immunol. *3*, 673–680.

Spergel, J.M., Mizoguchi, E., Brewer, J.P., Martin, T.R., Bhan, A.K., and Geha, R.S. (1998). Epicutaneous sensitization with protein antigen induces localized allergic dermatitis and hyperresponsiveness to methacholine after single exposure to aerosolized antigen in mice. J. Clin. Invest. *101*, 1614–1622.

Suh, P.G., Park, J.I., Manzoli, L., Cocco, L., Peak, J.C., Katan, M., Fukami, K., Kataoka, T., Yun, S., and Ryu, S.H. (2008). Multiple roles of phosphoinositide-specific phospholipase C isozymes. BMB Rep *41*, 415–434.

Wollenberg, A., Wetzel, S., Burgdorf, W.H., and Haas, J. (2003). Viral infections in atopic dermatitis: pathogenic aspects and clinical management. J. Allergy Clin. Immunol. *112*, 667–674.

Xiao, W., Hong, H., Kawakami, Y., Kato, Y., Wu, D., Yasudo, H., Kimura, A., Kubagawa, H., Bertoli, L.F., Davis, R.S., et al. (2009). Tumor suppression by phospholipase C-beta3 via SHP-1-mediated dephosphorylation of Stat5. Cancer Cell *16*, 161–171.

Xiao, W., Ando, T., Wang, H.Y., Kawakami, Y., and Kawakami, T. (2010). Lyn- and PLC-beta3-dependent regulation of SHP-1 phosphorylation controls Stat5 activity and myelomonocytic leukemia-like disease. Blood *116*, 6003–6013.

Yamamoto, N., Sugiura, H., Tanaka, K., and Uehara, M. (2003). Heterogeneity of interleukin 5 genetic background in atopic dermatitis patients: significant difference between those with blood eosinophilia and normal eosinophil levels. J. Dermatol. Sci. *33*, 121–126.

Yasudo, H., Ando, T., Xiao, W., Kawakami, Y., and Kawakami, T. (2011). Short Stat5-interacting peptide derived from phospholipase C-β3 inhibits hematopoietic cell proliferation and myeloid differentiation. PLoS ONE *6*, e24995.

Yoo, J., Omori, M., Gyarmati, D., Zhou, B., Aye, T., Brewer, A., Comeau, M.R., Campbell, D.J., and Ziegler, S.F. (2005). Spontaneous atopic dermatitis in mice expressing an inducible thymic stromal lymphopoietin transgene specifically in the skin. J. Exp. Med. *202*, 541–549.

Ziegler, S.F. (2012). Thymic stromal lymphopoietin and allergic disease. J. Allergy Clin. Immunol. *130*, 845–852.

Ziegler, S.F., and Artis, D. (2010). Sensing the outside world: TSLP regulates barrier immunity. Nat. Immunol. *11*, 289–293.

Supplemental Information

Critical role for mast-cell Stat5 activity in skin inflammation

Tomoaki Ando, Wenbin Xiao, Peisong Gao, Siavash Namiranian,

Kenji Matsumoto, Yoshiaki Tomimori, Hong Hong, Hirotaka Yamashita,

Miho Kimura, Jun-ichi Kashiwakura, Tissa R. Hata, Kenji Izuhara,

Michael F. Gurish, Axel Roers, Nicholas M. Rafaels, Kathleen C. Barnes,

Colin Jamora, Yuko Kawakami, and Toshiaki Kawakami

Content

Supplemental Figure S1. Eczematous *Plcb3*$^{-/-}$ mice exhibit high serum IgE, increased transepidermal water loss (TEWL) and strong fibrosis, Related to Figure 1. (A) Serum antibody levels in young and old WT and *Plcb3*$^{-/-}$ mice. (B)TEWL was measured on the shaved neck skin and back of young (6-7 weeks old) and old (7-10 months old) mice using Tewameter® TM 300 (CK electronic GmbH, Cologne, Germany). AD-like skin lesions were observed in the neck, but not back, skin of the old *Plcb3*$^{-/-}$ mice. (C) Skin lesions of spontaneously occurring dermatitis in *Plcb3*$^{-/-}$ (KO) and equivalent anatomical sites in WT mice were stained by Masson Trichrome. Blue staining represents deposition of collagen. Bar, 200 μm. Results in *A-C* are representative of 2 experiments using 3-5 mice per group.

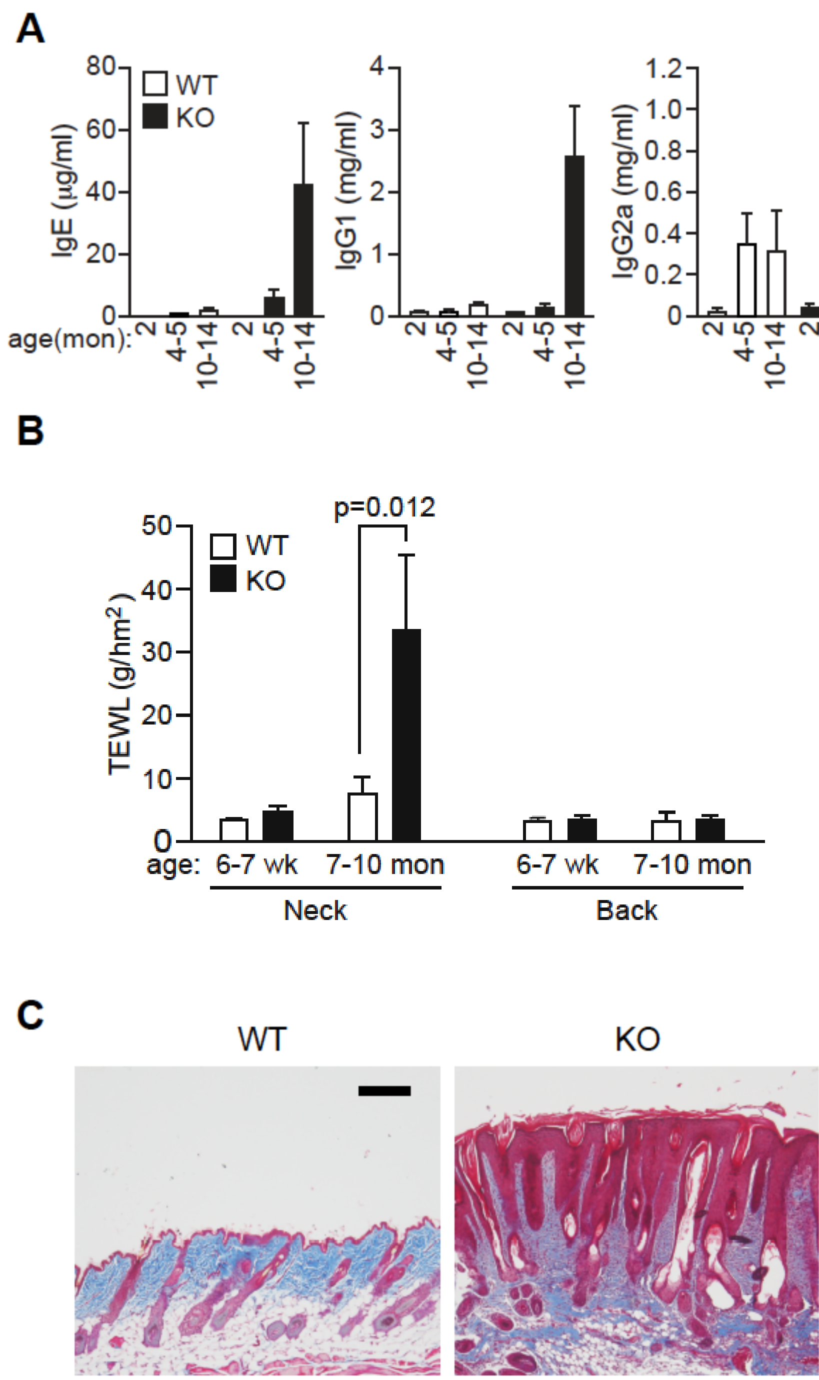

Supplemental Figure S2. Der f/SEB-stimulated *Plcb3$^{-/-}$* mice have similar levels of serum IgE and IgG1 compared to Der f/SEB-stimulated WT mice, Related to Figure 2. Total serum (A) and Der f-specific (B) immunoglobulins were quantified by ELISA on day 24 (see the Der f/SEB treatment schedule in Figure 2A). (C) AD scores with WT, *FceRIa$^{-/-}$* (a-), *Plcb3$^{-/-}$* (b3-), and *FceRIa$^{-/-}$;Plcb3$^{-/-}$* (a-;b3-) mice. Results in *A*-*C* are representative of 3 experiments using 3-6 mice per group.

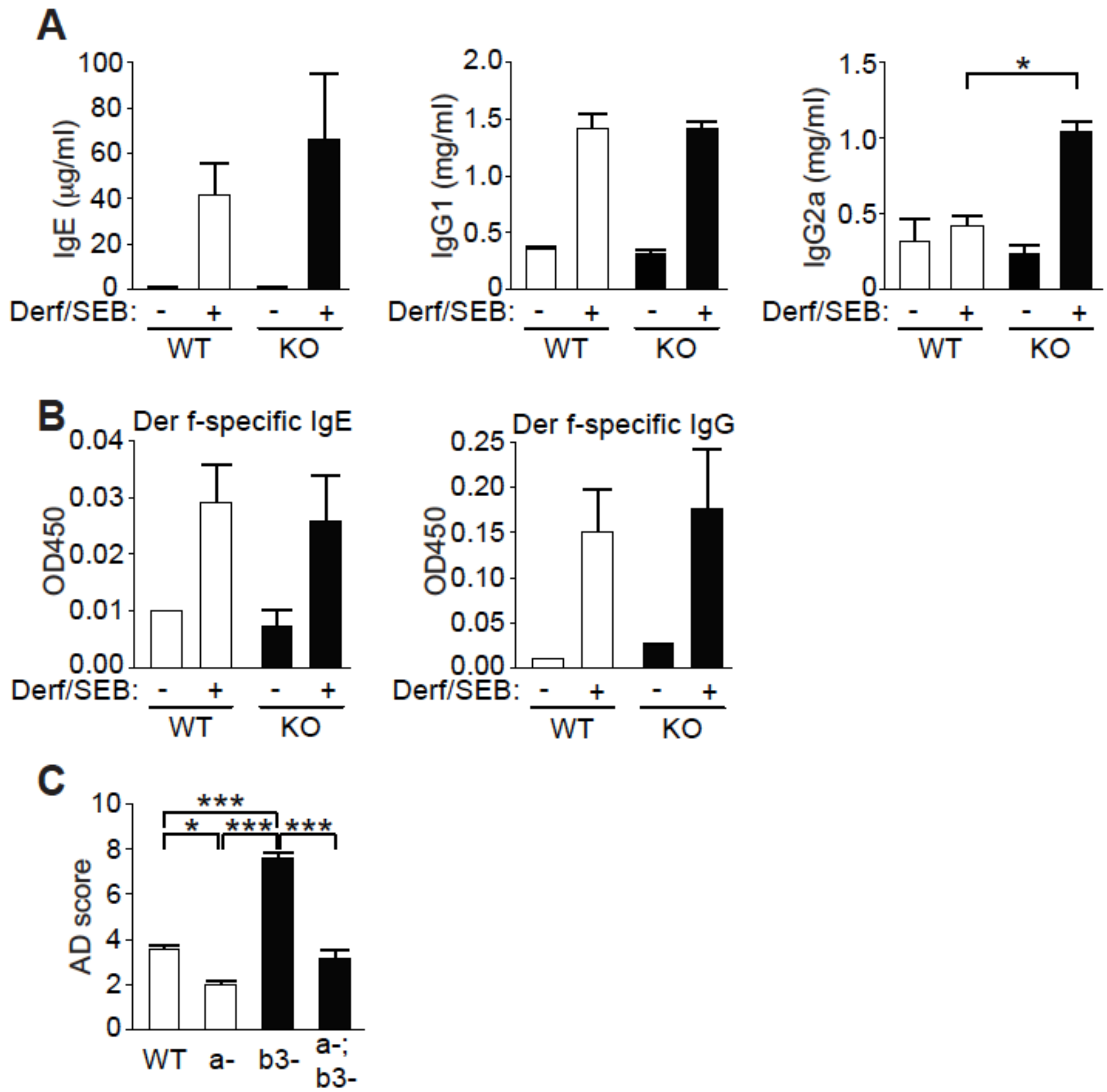

Supplemental Figure S3. ***Plcb3*$^{-/-}$ mice have increased BMCPs and MCPs whereas expression of IL-3 and IL-3R was comparable to WT mast cells, Related to Figure 3.** (A) Spleen and bone marrow cells from 10 week-old mice were analyzed by flow cytometry. Spleen cells were stained for c-Kit, FcγRII/III, integrin β7, and lineage markers, and c-Kit^{+}Lin^{-} cells were gated for detecting BMCPs. Lin^{-}Sca-1^{-}Ly6c^{-}FcεRI^{-}c-Kit^{+} bone marrow cells were gated for MCPs. *, $p<0.05$ vs. WT mice by Student's *t*-test. Results are representative of 2 experiments using 3 mice per group. (B) mRNAs for IL-3 or IL-3R components were quantified by microarray for ear skin tissues from 10 week-old WT and *PLC-β3*$^{-/-}$ mice (average of 4 mice each). (C) IL-3R on WT and *PLC-β3*$^{-/-}$ BMMCs was stained for flow cytometry.

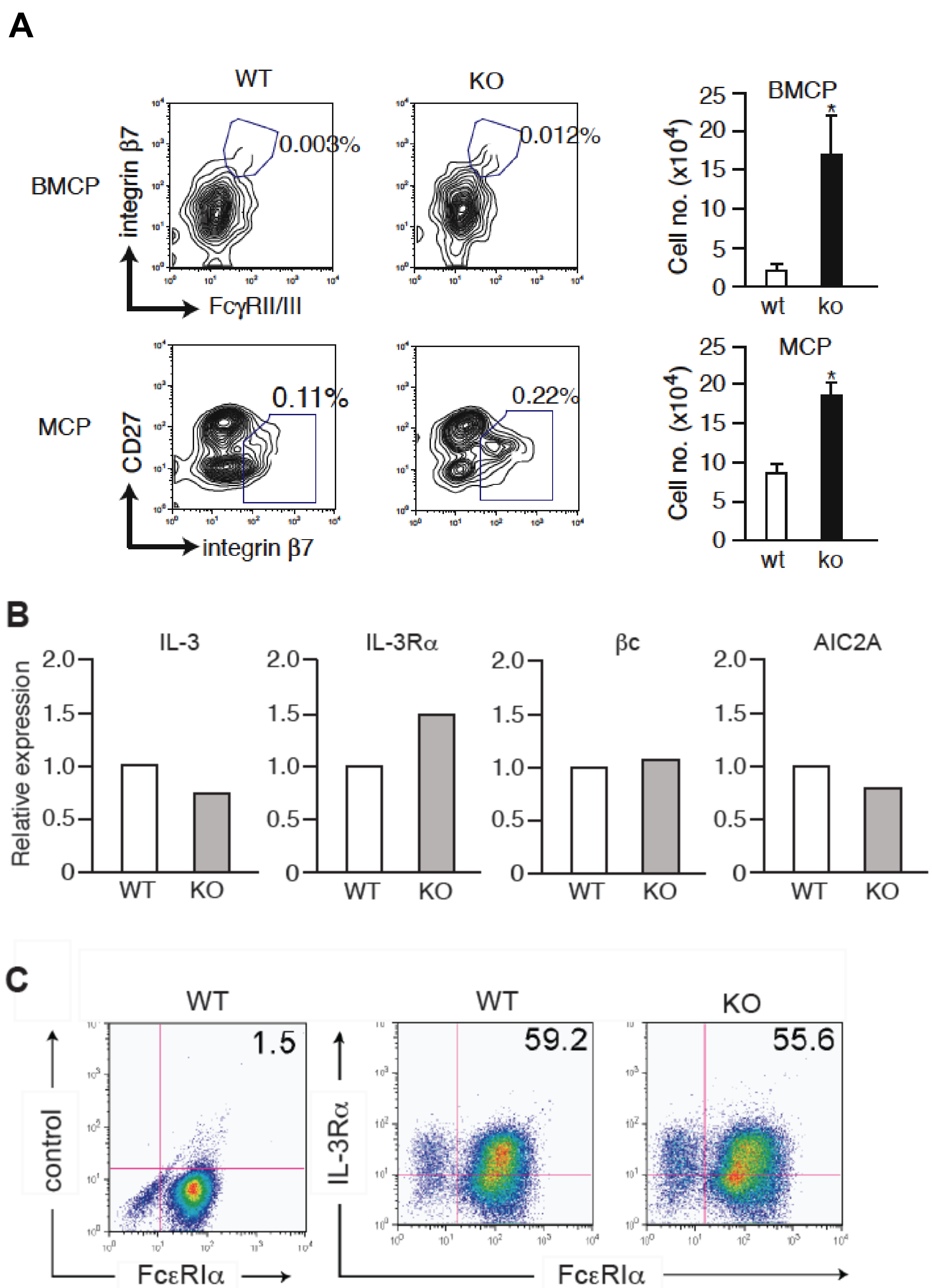

Supplemental Figure S4. Der f/SEB-induced AD scores are increased in *MCΔSHP-1* mice, while JAK Inhibitor TG101348 inhibits Der f/SEB-induced dermatitis, Related to Figure 4. (A-C) Dermatitis was induced with Der f/SEB in *MCΔShp1* mice (CKO or Cre(+)) and their floxed control (fl/fl or Cre(-)) mice. (A) Loss of expression of the targeted loci was confirmed by immunofluorescence microscopy of skin mast cells of MCΔShp1 (CKO) and control (fl/fl) mice. Arrowheads indicate mast cells. (B) Accumulated AD scores from 2 experiments. *, $p<0.05$ by Student's *t*-test. (C) Mast cells in the ears were stained with toluidine blue. HPF, high-power field. (D-H) B6 mice were co-treated epicutaneously with 100 μM TG101348 along with Der f/SEB. (D) AD scores. (E) Thicknesses of epidermis and dermis after Der f/SEB treatment. Veh, vehicle. (F) Histologic analysis of Der f/SEB-induced dermatitis. Immunofluorescence confocal microscopy was performed to detect TSLP (G) and periostin (H). Results in *D-H* are representative of 2 experiments using 3-5 mice per group.

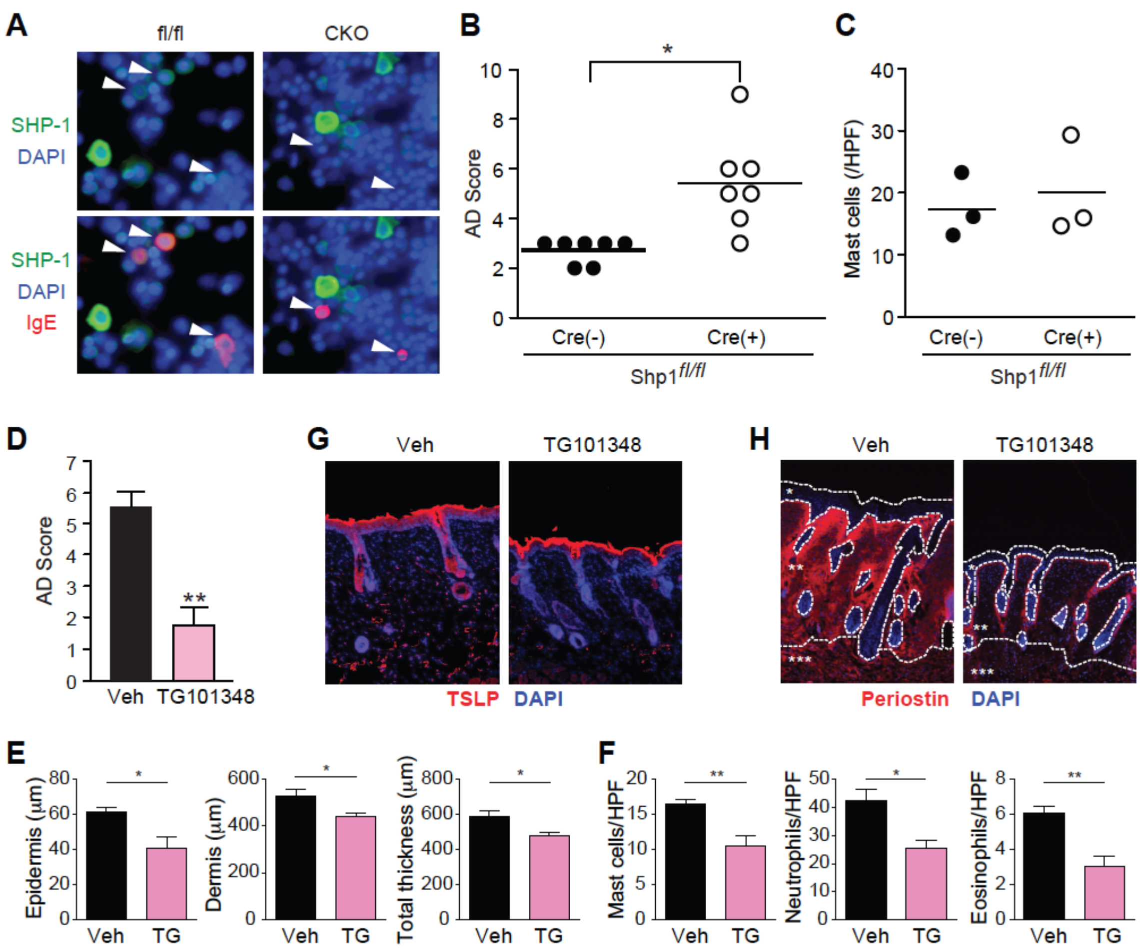

Supplemental Figure S5. TSLP expression in the skin and synergistic mast cell cytokine production by TSLP and FcεRI stimulation, Related to Figure 5. (A) Dermatitis was induced with Der f/SEB in WT, *Kit*$^{W\text{-}sh/W\text{-}sh}$, *Plcb3*$^{-/-}$, and *Plcb3*$^{-/-}$;*Kit*$^{W\text{-}sh/W\text{-}sh}$ mice. Lesional skin was stained for TSLP (red) and nuclei (blue). Borders of epidermis, dermis and subcutaneous fat tissues are indicated by dotted lines. (B) TSLP mRNA was quantified by qPCR with cultured keratinocytes derived from WT and *Plcb3*$^{-/-}$ mice. 18S RNA was used as a control. Results are representative of 2 experiments using 3 mice per group. (C) WT and *TSLPR*$^{-/-}$ (R-) BMMCs were sensitized with anti-DNP IgE and incubated with the indicated concentrations of antigen in the presence or absence of skin extract (Skin Ex) from WT mice. IL-13 and IL-6 secreted into culture media for 20 h were measured by ELISA. Note 1) that skin extract did not contain measurable amounts of IL-13 or IL-6, but skin extract alone induced cytokine production in BMMCs, 2) that antigen stimulation synergized with skin extract to induce cytokine production, and 3) that both IL-13 and IL-6 production induced by skin extract was lower by 20-30% in *TSLPR*$^{-/-}$ BMMCs than in WT BMMCs, except when BMMCs were stimulated with an optimal antigen concentration (10 ng/ml). Therefore, TSLP in skin extract enhances cytokine production by FcεRI-stimulated BMMCs. Essentially identical results were obtained using skin extract from Der f/SEB-treated skin (data not shown). *, $p<0.05$ by Student's *t*-test. Results in *C* are representative of 3 independent experiments.

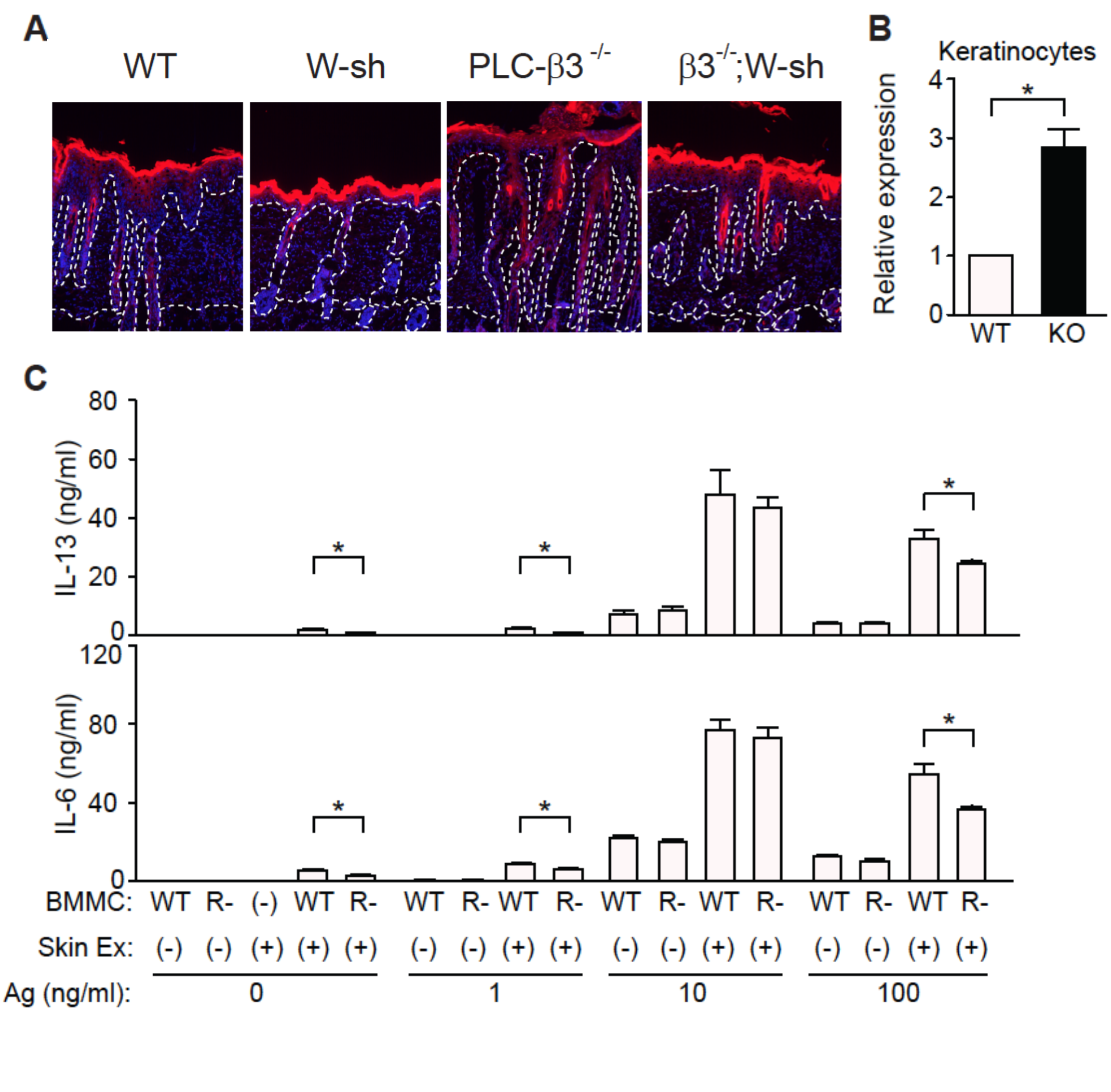

Supplemental Figure S6. Correlation between mast cell numbers and nuclear phospho-STAT5 levels in mast cells among human AD and healthy individuals and inverse correlation of STAT5 phosphorylation with PLC-β3 expression in mast cells in human skin, Related Figure 7. (A) SNP analysis on AD patients (ADEH+ and ADEH-) indicates an association of rs35169799 in *PLCB3* with log-transformed mean serum levels of total IgE (KU/L) in non-atopic European American subjects. (B) Pearson's correlation coefficients were calculated on the data in Figure 7. All data points were calculated (Total) or data points were divided into two groups based on the presence or absence of phospho-STAT5 upregulation in lesional mast cells. The results suggest the presence of two subsets of AD patients with vs. without increased phospho-STAT5 levels in lesional mast cells. **(**C) Skin samples of AD patients were stained for PLC-β3 (red), tryptase (green), and nuclei (blue). Representative images are shown from patient P4. (D-F) PLC-β3 levels in mast cells in lesional (L) and nonlesional (NL) skin samples of AD patients and healthy skin (H) were measured by Image J software (NIH). Skin sample from patient P2 was not available for this analysis due to sample shortage. (D) Data represent mean ± SEM. *, **, ***, ****: p<0.05, 0.01, 0.001, 0.0001 by Student's *t*-test. (E) Median of nuclear pSTAT5 intensity is plotted against that of PLC-β3 intensity. Linear regression curve (solid line) and the 95% confidence interval (dotted lines) are overlaid. Pearson's correlation is shown. (F) Nuclear pSTAT5 intensity in mast cells was compared between lesional and nonlesional skins. Patients are stratified by the presence or absence of a decrease of PLC-β3 expression in panel D. **, p<0.01; ****, p<0.0001 by Tukey's multiple comparison (ANOVA).

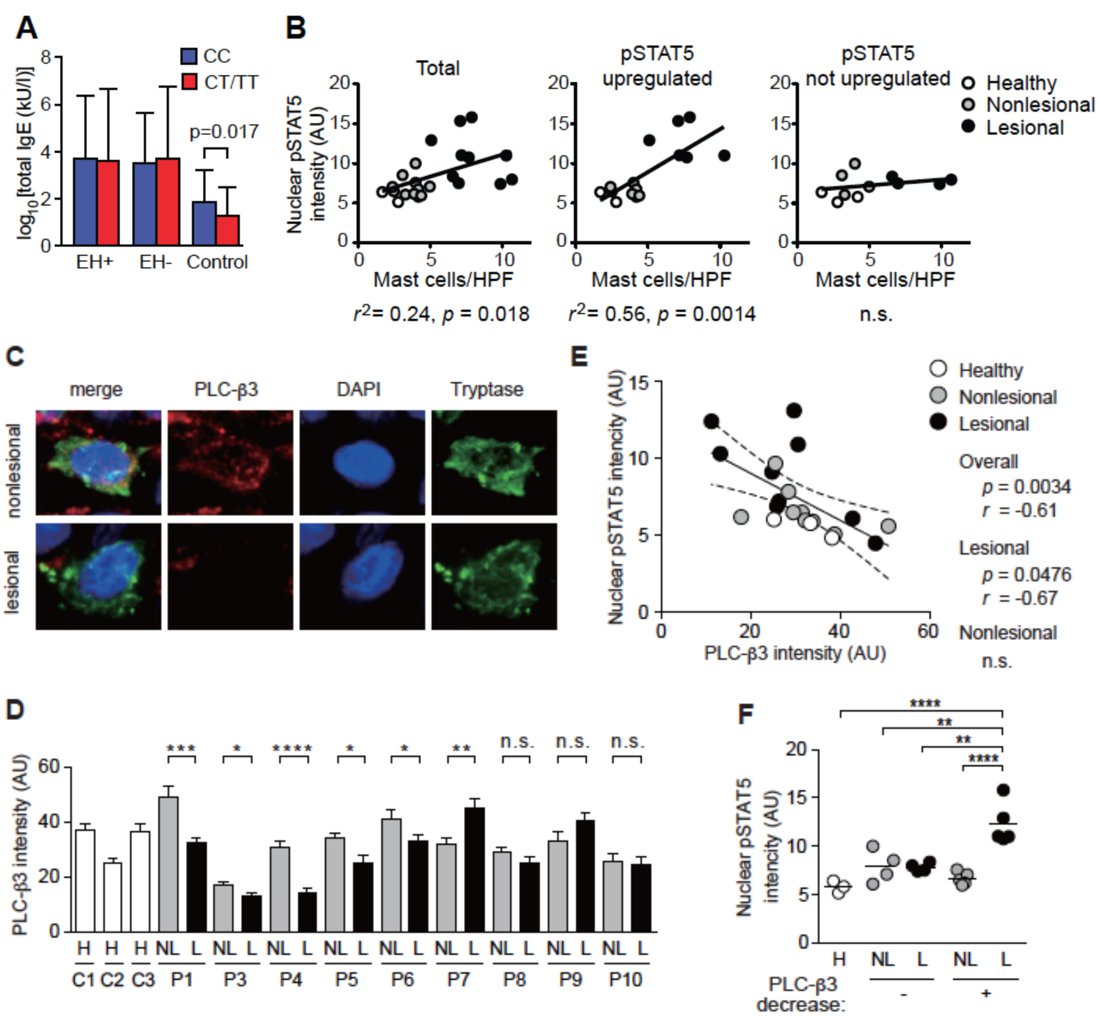

Supplemental Figure S7. Hypothetical vicious cycle of allergic skin inflammation consisting of T_H2 cytokines (secreted from T_H2 cells and mast cells)-periostin (secreted from fibroblasts)-TSLP and other proinflammatory cytokines (secreted from keratinocytes), Related to Figure 6. (A) Allergen-specific T_H2 cells stimulate production/secretion of periostin from fibroblasts. Then, periostin in turn stimulates keratinocytes to produce and secrete TSLP and other inflammatory cytokines. In this scheme, T_H2 cells seem to be required for initial epidermal overexpression of TSLP. Once sustained overexpression of TSLP is established, mast cells may play a more important role in persistent dermatitis than T_H2 cells. PLC-β3 can regulate activities of the cellular elements of this network, such as proliferation of mast cells, periostin production/secretion in fibroblasts and TSLP production/secretion in keratinocytes. Our data also suggest the presence of a feedback loop for inhibition of fibroblasts' periostin production by TSLP and PLC-β3 in fibroblasts is required for this feedback inhibition. DC, dendritic cell; T_H0, naïve $CD4^+$ T cells. (B) Model of SPS complex-mediated mast cell regulation. We showed that SHP-1 efficiently dephosphorylates Stat5 at Tyr^{694} in a PLC-β3-dependent manner in hematopoietic stem cells (Xiao et al., 2009) and mast cells (this study). Our study also showed that Lyn is another member of the SPS complex and that Lyn and SHP-1 regulate each other (Xiao et al., 2010). We propose that SPS members regulate mast cell biology (*e.g.*, proliferation) and AD pathogenesis.

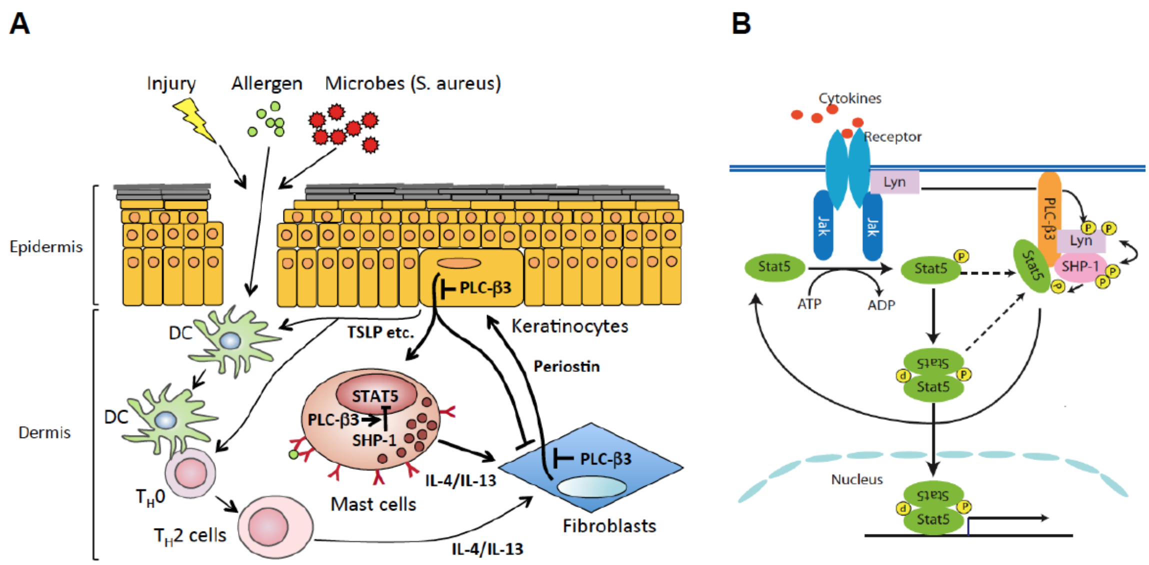

Supplemental Table S1. Similarity of gene expression profiles between spontaneous dermatitis in *Plcb3*$^{-/-}$ mice, Der f/SEB-induced dermatitis in WT mice and human AD, Related to Figure 7.

GEO accession	Orthologs common in the lists	Comparison	*Plcb3*$^{-/-}$ spontaneous skin lesion / WT normal skin		WT Der f/SEB-induced skin lesion / WT normal skin	
			Score	p-value	Score	p-value
GSE6012	10873	AD lesional / Normal skin	1252.7	<0.001	1198.9	<0.001
GSE5667	14325	AD lesional / Normal skin	952.5	<0.001	972.3	<0.001
GSE16161	10873	AD lesional / Normal skin	915.4	0.001	994.1	<0.001
GSE5667	14325	AD lesional / AD non-lesional	961.2	<0.001	1029.0	<0.001
GSE27887	14878	AD lesional / AD non-lesional	941.9	<0.001	1156.9	<0.001
GSE5667	14325	AD non-lesional / Normal skin	350.4	0.556	277.8	0.868
GSE26952	14889	AD non-lesional / Normal epidermis	913.5	<0.001	888.8	<0.001
GSE26952	14889	PS non-lesional / Normal epidermis	600.4	0.003	577.9	0.012

Similarity scores of gene expression changes in spontaneous dermatitis in *Plcb3*$^{-/-}$ mice (vs. normal skin in WT mice), Der f/SEB-induced dermatitis in WT mice (vs. normal skin in WT mice) and human AD (the indicated matches in Comparison column) were computed by OrderedList algorithm. Numbers of the orthologs compared, similarity scores and p-values are shown. For comparison, data with Der f/SEB-induced skin lesions (Ando et al., 2013) and human psoriasis are included.

Supplemental Table S2. SNP identities, location and minor allele frequency in PLCB3, STAT5A, STAT5B and SHP1, Related to Figure 7

Gene (Chromosome)	dbSNP ID	Location	Type of Variant	Risk allele	Allele frequency	
					European American (N=156)	African American (N = 152)
PLCB3	rs2244625	63782720	Coding exon	G	0.328	0.772
(11q13.1)	rs915987	63784464	Intron	A	0.141	0.030
	rs35169799	63787817	Coding exon	T	0.057	0.020
	rs3815362	63790131	Intron (boundary)	T	0.340	0.093
STAT5A	RS16967637	37699948	Intron	A	0.349	0.391
(17q21.2)	RS7217728	37700927	Intron	T	0.652	0.366
	RS13380828	37701981	Intron	A	0.010	0.259
	RS9906989	37709372	Intron	T	0.181	0.173
	RS2272087	37713088	Intron (boundary)	G	0.187	0.254
	RS2293154	37714529	Intron (boundary)	T	0.186	0.171
STAT5B	rs17500235	37609886	Intron	C	0.056	0.010
(17q21.2)	rs9900213	37629407	Intron	A	0.206	0.541
	rs6503691	37647616	Intron	A	0.138	0.612
	rs17591972	37652970	Intron	G	0.103	0.185
SHP1	RS7310161	6927395	Promoter	A	0.560	0.204
(12p13.31)	RS7966756	6932652	Intron	A	0.063	0.454
	rs10744724	6935542	Intron	C	0.059	0.507
	RS759052	6939881	Intron (boundary)	T	0.122	0.431

Supplemental Table S3. Demographic characteristics of AD and control populations, Related to Figure 7

Characteristics	European American		African American	
	AD	Healthy	AD	Healthy
No. of subjects	248	156	171	152
Males; N (%)	91 (36.7%)	63 (40.4%)	40 (23.4%)	77 (50.7%)
Age (yr); mean (SD)	33.1 (18.5)	36.6 (13.2)	35.3 (12.5)	41.1 (10.3)
Geometric mean IgE levels (95%CI)	694.1 (522-922)	59.1 (48-111)	504.8 (378-1229)	141.2 (113-299)
Geometric EASI score (95%CI)†	4.6 (3.9-5.4)	NA	3.7 (3.0-4.5)	NA

The following abbreviations used are: AD, atopic dermatitis; EASI, eczema area and severity index; and NA, not applicable. †EASI score is determined by the percentage of eczema area on a 7-point ordinal scale: 0 =<10%; 1=10%-29%; 3=30%-49%; 4=50%-69%; 5=70%-89%; and 6=90%-100%.

Supplemental Table S4. Association between SNPs in PLCb3, STAT5A, STAT5B and SHP1 and AD and related phenotypes, Related to Figure 7

Gene and SNP	Position (Mb)	Risk allele	AD				ADEH				EASI	
			European American		African American		European American		African American		African American	
			OR (95%CI)†	P	OR (95%CI)	P	OR (95%CI)	P	OR (95%CI)	P	Beta	P
PLCB3												
rs2244625	63.783	G	1.03 (0.72, 1.48)	0.87	0.98 (0.66, 1.44)	0.904	1.62 (1.06, 2.48)	**0.027***	0.82 (0.33, 2.05)	0.678	0.028 (-0.14, 0.19)	0.738
STAT5A												
rs16967637	37.7	A	0.74 (0.53, 1.04)	0.08	0.91 (0.63, 1.31)	0.609	0.83 (0.54, 1.29)	0.411	1.31 (0.63, 2.74)	0.466	0.151 (0.00, 0.30)	**0.048**
STAT5B												
rs9900213	37.629	A	0.66 (0.44, 99)	**0.045**	0.87 (0.61, 1.24)	0.448	1.4 (0.86, 2.30)	0.18	1.74 (0.76, 3.99)	0.191	0.075 (-0.07, 0.22)	0.32
SHP1												
rs7310161	6.927	T	1.55 (1.10, 2.17)	**0.012**	1.32 (0.86, 2.03)	0.207	1.05 (0.72, 1.54)	0.694	0.85 (0.34, 2.13)	0.735	-0.226 (-0.40, -0.05)	**0.012**
rs7966756	6.933	A	0.9 (0.47, 1.73)	0.756	1 (0.71, 1.41)	0.99	0.9 (0.38, 2.11)	0.802	1.04 (0.52, 2.08)	0.922	-0.227 (-0.36, -0.10)	**0.0009**
rs10744724	6.935	C	0.95 (0.49, 1.83)	0.875	1.26 (0.90, 1.78)	0.183	0.76 (0.31, 1.87)	0.553	0.72 (0.34, 1.50)	0.376	-0.258 (-0.39, -0.12)	**0.0003**
rs759052	6.94	T	1.07 (0.66, 1.75)	0.785	1.3 (0.92, 1.84)	0.139	0.69 (0.36, 1.34)	0.272	0.42 (0.22, 1.14)	0.101	-0.241 (-0.38, -0.10)	**0.001**

*P=0.006 when analysis was done in a recessive model.

†Allelic odds ratios